Summer 2017

Characterization of a Thermoresponsive Water-Soluble Polymer: Block-Copoly [Ethylene Glycol/ Graft-Co (Vinyl Alcohol/Vinyl Caprolactam)]

Adebola Margaret Adeleni
Missouri State University, Adebola227@live.missouristate.edu

CHARACTERIZATION OF A THERMORESPONSIVE WATER-SOLUBLE POLYMER: BLOCK-COPOLY [ETHYLENE GLYCOL/GRAFT-CO (VINYL ALCOHOL/VINYL CAPROLACTAM)]

A Masters Thesis

Presented to

The Graduate College of

Missouri State University

In Partial Fulfillment

Of the Requirements for the Degree

Master of Science, Chemistry

By

Adebola Margaret Adelani

August 2017

CHARACTERIZATION OF A THERMORESPONSIVE WATER-SOLUBLE POLYMER: BLOCK-COPOLY [ETHYLENE GLYCOL/GRAFT-CO (VINYL ALCOHOL/VINYL CAPROLACTAM)]

Chemistry

Missouri State University, August 2017

Master of Science

Adebola Margaret Adelani

ABSTRACT

Thermoresponsive polymers are a class of smart materials that exhibit change in their physical properties with temperature, which make them unique and useful materials in a wide range of biomedical applications. Soluplus®, a thermoresponsive block graft copolymer with poly(vinyl acetate) PVAc and poly(vinyl caprolactam) PVCL block grafted on a poly(ethelyne glycol) PEG backbone in a ratio of 30:57:13 respectively, is marketed by BASF Corporation, it aids in solubilizing and increasing the bioavailability of active Pharmaceutical ingredients in poorly water soluble drugs. In order to elucidate the effect of hydrophobic/hydrophilic balance on thermoresponsive behavior of Soluplus® in water. Soluplus® was hydrolyzed by methanolysis, which resulted in the quantitative conversion of PVAc to poly(vinyl alcohol) PVOH. NMR and IR spectroscopies were used to confirm the structure of the hydrolyzed sample. The cloud-point of the hydrolyzed sample was found to be lower than that of Soluplus®. Expectedly, the gelation temperature and concentration of the hydrolyzed was higher than that of Soluplus®, which was attributed to its hydrophilicity. The micelle size distribution was random and larger compared to those of the Soluplus® parent compound.

KEYWORDS: Soluplus®, thermoresponsive, methanolysis, cloud-point, gel point, phase diagram, micelle size distribution, active pharmaceutical ingredient.

This abstract is approved as to form and content

_____

G. Alan Schick, PhD
Chairperson, Advisory Committee
Missouri State University

CHARACTERIZATION OF A THERMORESPONSIVE WATER-SOLUBLE POLYMER: BLOCK-COPOLY [ETHYLENE GLYCOL/GRAFT-CO (VINYL ALCOHOL/VINYL CAPROLACTAM)]

By

Adebola Margaret Adelani

A Masters Thesis
Submitted to the Graduate College
Of Missouri State University
In Partial Fulfillment of the Requirements
For the Degree of Master of Science, Chemistry

August 2017

Approved:

_____
G. Alan Schick, PhD

_____
Reza Sedaghat-Herati, PhD

_____
Keiichi Yoshimatsu, PhD

_____
Mahua Biswas, PhD

_____
Julie Masterson, PhD: Dean, Graduate College

ACKNOWLEDGEMENTS

I would like to thank my family for their continuous support towards my graduate program.

I would to thank my research advisor Dr. Alan Schick for his assistance in and outside the lab, for his patience, motivation and guidance throughout my entire time of research and writing of this thesis.

I would like to thank Dr. Reza Sedaghat-Herati and Dr. Adam Wanekaya for their time and help in the lab.

I would like to thank Dr. Santimukul Santra, Pittsburg State University, for MALDI-TOF analysis.

I would like to thank the rest of my thesis committee, Dr. Reza Sedaghat-Herati, Dr Keiichi Yoshimatsu, and Dr. Mahua Biswas, for their time, patience and their intellectual contributions to this thesis.

I would like to thank the Chemistry Department faculty and staff for their support during the course of my graduate studies.

I dedicate this thesis to Almighty God

TABLE OF CONTENTS

LIST OF TABLES

LIST OF FIGURES

1. INTRODUCTION

1.1 Thermoresponsive Polymers

Stimuli-responsive or "smart" materials - have the ability to respond to external stimuli and represent one of the most exciting and immerging class of materials.[1] They have found wide acceptance across a variety of fields due to their ability to exhibit significant change in physicochemical properties as a result of a small change in their environment, such as temperature, light, pH, electric potential, magnetic and ionic field, pressure, redox.[1,2] One of the major groups of these materials is based on polymers because of their many advantages.

Polymer solutions with stimuli-responsive properties such as fast and reversible conformational or phase change in response to variations in temperature are referred to as thermoresponsive polymers.[3] A veriety of these polymers have been studies over the past few decades, some of which are poly(*N*-alklyacrylamide)s,[4] poly(*N*-vinyl caprolactam),[5] poly(methyl vinyl ether),[6] poly(*N*-ethyl oxazoline).[7]

According to Hou,[8] these polymers are divided into three main categories: The thermo-induced shaped memory polymers, which are polymers with high glass transition temperature and are able to change their hard phase with induced temperature change; liquid crystalline elastomers, which combine the properties of both polymeric elastomer and liquid crystals;[9] lastly we have those that undergo liquid-liquid phase transition in response to temperature change,[8] which is the focus of this thesis project.

1.2 Phase Transition In Thermoresponsive Polymer Solutions

Thermoresponsive polymers in aqueous solutions exhibit a critical solution temperature, where phase separation is induced by a small change in temperature. The temperature at which the polymer solution starts to phase-separate, thus becomes cloudy is known as cloud point. The different types of phase transition diagrams associated with cloud point that occur in this type of polymer are schematically depicted in Figure 1, namely lower critical solution temperature (LCST), upper critical solution temperature (UCST), and closed loop coexistence of LCST and UCST.[10] Figure 1a, 1b and 1c shows the bimodal curves for polymer solutions exhibiting LCST, UCST and both LCST and UCST.

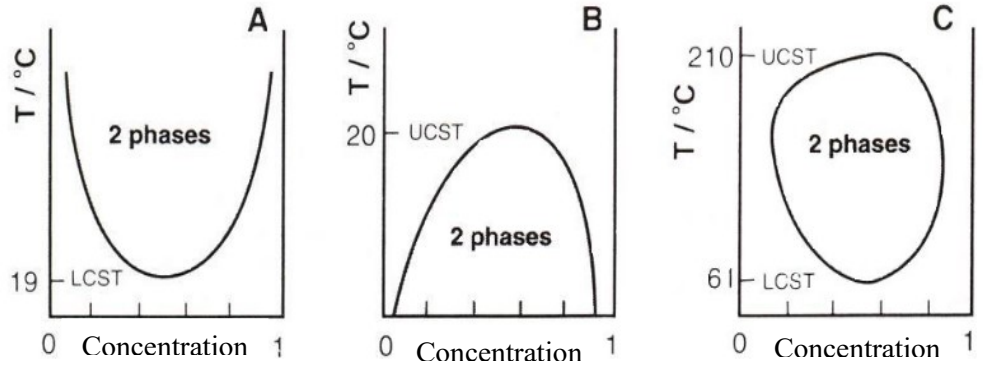

Figure 1: The three (most common) types of phase diagrams that exist in polymer-aqueous system a) LCST, b) UCST, c) Coexistence of both LCST and UCST.[10]

1.2.1 Lower Critical Solution Temperature (LCST) Behavior. Polymer solutions with LCST behavior are highly soluble, typically in water, but become insoluble as the temperature of solution increases. Above cloud point, aggregation of the polymer chain

results in turbidity.[11] It is often referred to as the coil-globule (C-G) transition because of changes occurring in the structure of the polymer backbone.[12] From thermodynamic point of view, this means that the free Gibbs energy ($\Delta G = \Delta H - T\Delta S$) of dissolving the polymer in water is negative at lower temperature and positive at higher temperature. Such behavior is possible if the enthalpy of hydrogen bonding between water molecules and the polymer chains (ΔH) and the entropy contribution (ΔS) are both negative. That is, if water loses entropy when it hydrates the polymer chains, then as the temperature of the system is raised, the entropy term ($-T\Delta S$) will come to dominate the process and produce a positive Gibbs free energy of mixing. This will lead to phase separation.[10,12,13] This transition is typically reversible, providing access to sharp, reversible temperature-induced phase transition.

A wide variety of thermoresponsive polymers has been studied over the years. Poly(*N*-isopropyacrylamide) belongs to class *N*-substituted acrylamides, which has attracted a lot of interest due to their unique phase behaviors in aqueous media.[14] Poly(*N*-isopropyacrylamide) was the first reported and has been the most extensively studied amongst them.[10,14] The LCST of poly(*N*-isopropyacrylamide) is of great interest bio-medically and technologically because of its proximity to human body temperature (cloud point temperature at 32 °C), thus applications in controlled drug delivery have been studied.[15]

Another well characterized polymer of this type is poly(*N*-vinyl caprolactam), which also shows LCST in the range of physiological temperatures.[16] Table 1 shows some examples of homo-polymers with LCST behavior in aqueous solution and their corresponding phase transition temperatures.[10,16,17,18,19]

Table 1: Some examples of thermoresponsive polymer that exhibits LCST behavior in aqueous solutions.

Name of Polymer	Abbreviation	LCST (°C)	Reference
Poly(*N*-isopropylacrilamide)	PNIPAM	30-34	17
Poly(*N*,*N*-diethylacrylamide)	PDEAAM	32-34	17
Poly(*N*-vinylcaprolactam)	PVCL	30-33	16
Poly(methyl vinyl ether)	PMVE	34	10
Poly(*N*-cylopropylacrylamide)	PNCPAM	47	18
Poly(ethylene oxide)s and Poly(prolylene oxide)s	PEO & PPO	15	19

1.2.2 Upper Critical Solution Temperature (UCST) Behavior. In contrast, polymer in aqueous solutions that show UCST-type phase behavior are uncommon. They are those with positive temperature dependence which exhibits phase separation below cloud point, in other words they are insoluble in solvent, but becomes soluble with increase in temperature. In many cases, UCST phase transition occurs when solute-solute and solvent-solvent interaction dominates the solute-solvent interaction to generate a positive enthalpy of mixture.[20] In order to explain the UCST behavior, consider the enthalpic term (ΔH) to represents the supramolecular interaction of the polymer chains in the Gibbs free energy equation, however, the supramolecular Interaction strength decreases with increase in temperature, which make the hydration term dominate and leads to polymer dissolution. The polymer itself must be very hydrophilic in order to make its UCST transition greater than its potential LCST transition which leads to

complete insolubility.[10] An example of a UCST-type of polymer is the mixture of poly(acrylic acid) and poly(acrylamide) in water which is triggered by hydrogen bonds between the carboxy groups and amide groups.[21] Another example, first reported in 1967, is poly(*N*-acryloylglycinamide). In this case, the phase separation is triggered by inter and intramolecular formation of hydrogen bonds in the amide groups.[22] Thus, UCST behavior can be produced by either hydrogen bonding or electrostatic interactions. Table 2, represent some examples of thermoresponsive polymers with UCST behavior in aqueous solution and their corresponding phase transition temperatures.[17,22,23,24]

Table 2: Some examples of thermoresponsive polymers that exhibits UCST behavior in aqueous solutions.

Name of Polymer	**Abbreviation**	**UCST (°C)**	**Reference**
Polyacrylamide and polyacrylic acid	PAAm/PAA	25	17
poly(*N*-acryloylglycinamide)	PNAGA	13-22	22
Poly(vinyl methyl ether)	PVME	-21	23
Poly(allylurea) and Derivatives	PU	16-46	24

1.2.3 Polymer with Both LCST and UCST Behavior. Double thermoresponsive polymers that exhibit LCST and UCST behavior in aqueous media are also attractive because they offer a very good potential to engineer smart materials that can respond only within a specific range of environmental conditions.[25] This type of polymers either be achieved by copolymerization or modification of an already existing block copolymer.

An example compound is a triblock copolymer of 2-(2-methoxyethoxy)ethyl methacrylate (MEO_2MA), oligo(ethylene glycol) methacrylate (EO_2MA), and *N*-[3-(dimethylamino) propyl] methacryl-amide (DMAPMA) synthesized by Tian, *et al*.[26] This block copolymers exhibit double thermoresponsive behavior, where the poly(MEO_2MA-*co*-EO_2MA) block produces LCST behavior, and the DMAPMA block produces UCST behavior.

Another example of this was demonstrated by Kafer, *et al*.[27] who synthesized poly(ethylene glycol)-*b*-poly(acrylamide-*co*-acrylonitrile). This copolymer exhibits double thermoresponsivity, in which the UCST-type behavior was attributed to the phase transition of the UCST-type of an acrylamide-co-acrylonitrile copolymer while the LCST responsive behavior by the inclusion of the poly(ethylene glycol) block. Table 3 below shows more examples of graft/block copolymers with both LCST and UCST in aqueous media.[28,29,30]

1.3 Sol-gel Transition.

Another basic feature of thermoresponsive polymers is that they can undergo transition from a solution phase (flowing fluid) to a gel phase (non-flowing). This process is dependent on temperature and concentration and is also referred to as the sol-gel transition. Above the critical concentration (critical gel concentration) of the polymer, the gel phase appears (gel point).[31] This can be achieved either by chemical and/or physical crosslinking.[32] In this project only the latter is addressed.

Physical crosslinking relies on temporary reversible hydrophobic interactions, hydrogen bonding, ionic interactions etc.[32,33] When the solvent is water, the interaction between

polymer and water is governed by hydrogen bonding and hydrophobic interactions with water molecules, as seen in Figure 2.

Table 3: Some examples of thermoresopnsive graft/block copolymers from literature and their corresponding LCST and UCST.

Name of Polymer	**Abbreviation**	**LCST & UCST (˚C)**	**Reference**
Poly(*p*-dioxanone)graft-poly(vinyl alchol)	PVA-g-PPDO	30 & 80	31
Poly(vinylidene fluoride)-graft-poly(diethylene glycol methyl ether methacrylate)	$PMeO_2MA$-g-PVDF	23 & 27.5	32
Poly[oligo(ethylene glycol) methyl ether methacrylate-block-poly(*N*-isopropylacrylamide)	POEGMA-b-PNIPAM	15 & 25	33

Because this physical crosslinking relies on temporary reversible network formation, the thermo-gelling phenomenon is typically reversible.[34] Hence, it may not be as stable as it would be if it were chemically crosslinked.[34] In other words, the viscosity of the polymer solution increases when the temperature is raised, and at critical temperature (and at critical gel concentration) it forms a hydrogel. Hydrogel can then return to a solution phase by lowering the temperature.

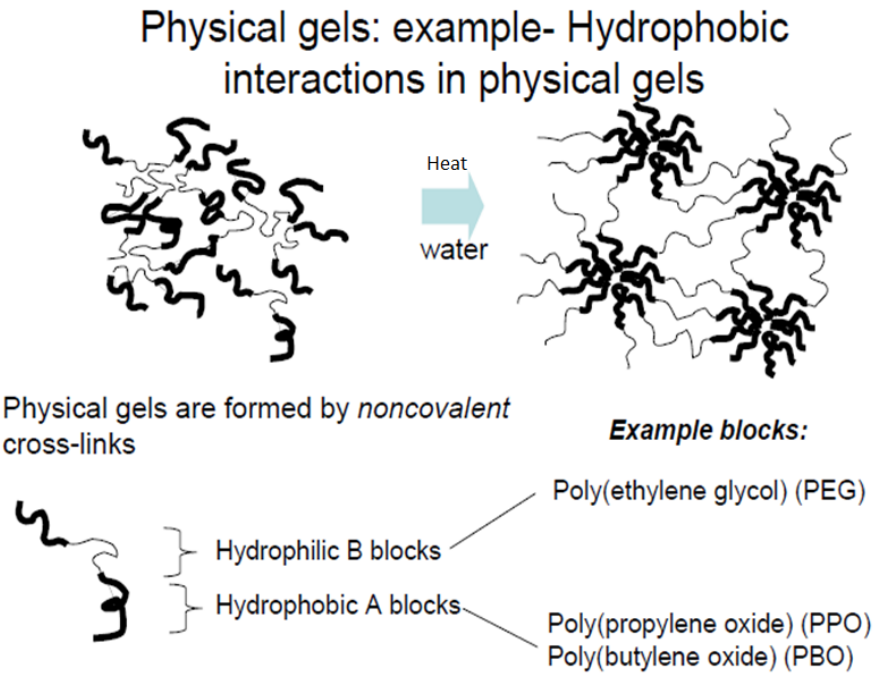

Figure 2: The formation of physical gels by crosslinked hydrophilic polymer network in aqueous media.[35]

1.4 Amphiphilic Block Copolymers and Micelle Formation

Amphiphilic block copolymers often show self-assembly behavior. When amphiphilic block copolymer (polymers with both hydrophobic and hydrophilic block properties) are dissolved in aqueous media, the different blocks of the copolymer have different affinities for the solvent, one being hydrophobic and the other hydrophilic.[36] As a result, polymeric micelles ranging from tens to hundreds of nanometers in diameter are formed. These are colloidal systems composed of amphiphilic polymers that self-assemble above the critical micelle concentration (CMC) to form specific core-corona structures,[37] similar to the classical structure shown in Figure 3, in which the hydrophilic portions are in contact with water (corona), and the hydrophobic moieties are gathered in the core to minimize their contact with water.[38]

In self-assembly process, the transfer of the dispersed copolymer to the micellar core is attributed to changes in the state of dilution and deformation of the hydrophobic block. Secondly, the hydrophilic block is transferred to the corona region of the micelle, this is also as a result of changes in the state of dilution and deformation in the hydrophilic block. Thirdly, the formation of micelle localizes the copolymer such that the hydrophobic block is confined to the core while the hydrophobic is confined to the corona. Lastly, the formation of the micelle is associated with the establishment of an interface between the micelle core made up of the hydrophobic block and the corona consisting of the hydrophilic block and the solvent.[36]

The main driving force of this self-assembly associated with these polymers is their hydrophobicity. These micelles can incorporate a reasonable amount of hydrophobic materials, which is essential for biomedical applications. Sizes and size distribution of this nanoparticles at different concentrations also play an important role in drug delivery systems.

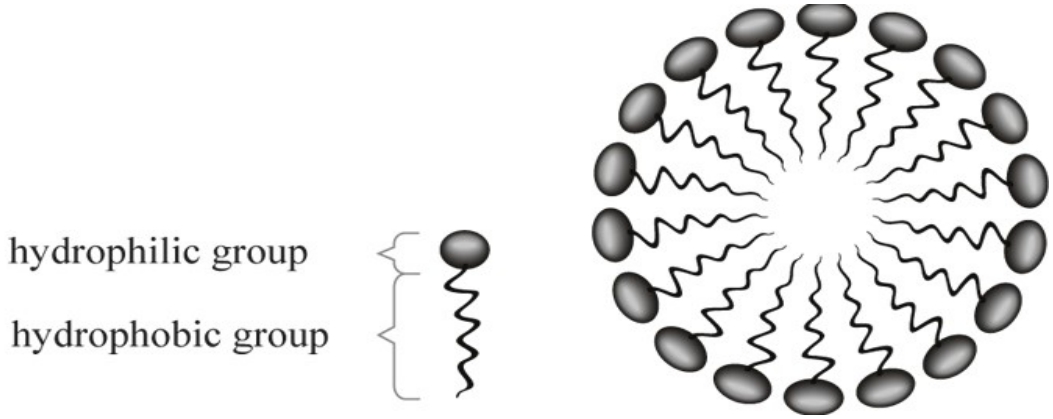

Figure 3. Classical micelle structure layout.[39]

1.5 Some Applications of Thermoresponsive Polymers.

Based on their unique properties, thermoresponsive polymers provide a promising basis for the development of smart materials. The aim in this section is to discuss recent examples in order to highlight these potentials.

Polymers that show cloud point temperatures in the proximity of human body temperature allow self-assembly architectures which are useful for biomedical applications. Recently, attention has been drawn towards polymer drug, gene, and radionuclide delivery systems.[40] Some radionuclide delivery systems are used in connection with polymers because they may serve *in vivo* for tacking bio-distribution in imaging techniques such as positron emission topography (PET).[40] Thus, in many applications, the polymers come in contact with ionizing radiation, especially when they are used as carriers for radiopharmaceuticals.

As illustrated by Sedlacek, *et al*.[40] poly(2-isopropyl-2-oxazoline-*co*-2-*n*-butyl-2-oxazoline) (POX) is radio-resistance, poly(*N*-isoprpylacrylamide) is only suitable for low radiation demand while poly(*N*-vinlycaprolactam) showed the least resistance to radiation.

The controlled conformational and thermodynamic changes of thermoresponsive polymers can also be exploited for their potential use in cell culture. This application involves the formation of switchable substrates by coating the surface with a thermoresponsive polymer.[41] Here, liver epithelial cells (LE_2) were cultured on polymeric surface printed with Jeffamine/ *N*,*N*-diethylacrylamide hydrogel, which showed that LE_2 cells adhere selectively to the polymer features and that any changes in the cell behavior can be monitored with changing temperature.[41]

In addition to the applications based on temperature sensitivity, thermoresponsive polymers can also be used to reduce enzyme cost in the production of lignocellulosic biofuels.[42] In this study, highly adaptable thermoresponsive polymer-protein bio-conjugates were developed through free radical copolymerization of *N*-isopropylacrylamide and *N*-isopropylmethylacrylamide with an alkoxyl-amine bearing methylacrylamide in the presence of azobisisobutyronitile (AIBN) as the initiator, the two copolymers exhibit LCSTs of 42.5 ºC and 58.1 ºC respectively. Hyper-thermophilic enzyme endoglucanase, an enzyme which converts the cellulose components of lignocellulosic into fermentable sugars for biofuel production, was incorporated into the copolymer *via* the N-terminus. When the cellulosic substrate is added, it is degraded by the bio-conjugate, the temperature of the solution is raised above LCST to precipitate the cellulase, the soluble oligosaccharide product is removed, and the temperature is the lowered below LCST to resolubilize the cellulase, to continue the circle. This process is repeated to continue the cycle. Other applications include gene delivery, tissue engineering, glucose sensors.[17]

1.6 Soluplus®

Soluplus®, a polymeric solubilizer with an amphiphilic chemical structure, is marketed as an excipient that enables new levels of solubility and bioavailability for poorly soluble active pharmaceutical ingredients.[43] Soluplus® is a polyvinyl caprolactam (PVCL)-polyvinyl acetate (PVAc)-polyethelene glycol (PEG) triblock graft copolymer, with an average molecular weight in the range of 90,000 to140,000 g/mol and monomer ratio of 57:30:13 respectively.[44] The structure of Soluplus® is shown in Figure 4. The

PEG 6000 hydrophilic block is the polymer backbone with one or two side chains PVAc randomly copolymerized with PVCL.[45]

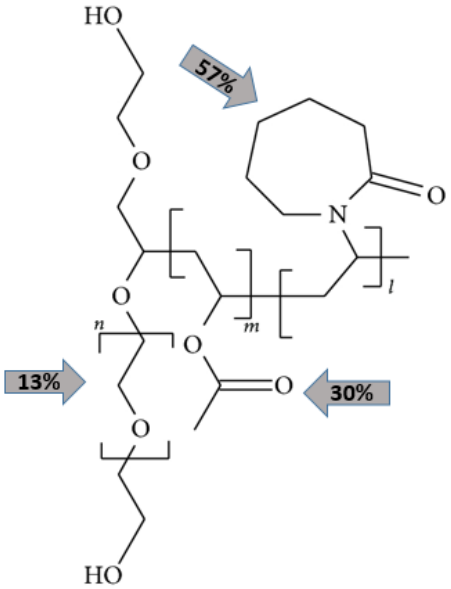

Figure 4. The structure of Soluplus®. The three blocks, PVCL, PVAc, PEG and their respective monomer ratios 57:30:13.[44]

The composition of Soluplus® (Figure 4) allows the polymer molecule to self-assemble and to form molecular micelles. The structure also results in concentration-dependent sol-gel and cloud point phase transitions in aqueous media. The cloud point temperature of Soluplus® is in the range of physiological relevant temperature (28-31 ° C) and thus another potential compound for biomedical applications.

1.7 Research Objectives

Varying the ratio of hydrophobic and hydrophilic chain length in amphiphilic block copolymers often alters thermoresponsive properties of such copolymers.[46,47,48,49]

For instance, the decrease of cloud point temperature upon increase of hydrophobic ratio has also been observed in literatures for thermoresponsive systems based on PNIPAM.[47] The aim of this research is to explore similar trends for thermoresponsive polymers based on PVCL, beginning specifically with a Soluplus® derivative:

- To hydrolyze Soluplus®, thus, converting PVAc (hydrophobic) block to PVOH (hydrophilic).

- To evaluate the effect of this conversion on the thermoresponsive properties of Soluplus® in terms of cloud point, gel point and micelle size distribution of the hydrolyzed analog, PEG-PVOH-PVCL.

2. EXPERIMENTAL

2.1 Materials

Soluplus® was provided by BASF Corporation and used without further purification. Methanol (CH_4O, HPLC Grade) and potassium hydroxide (KOH) were purchased from Fisher Scientific and used without further purification. Potassium bromide (KBr, FT-IT grade) and dimethyl sulfoxide-d_6 were purchased from Sigma-Aldrich and used without further purification. Float-A-Lyzer® dialysis tubes with molecular weight (cut-off: 500-1000 Da) were purchased from Spectrum laboratories, Inc. Polystyrene cuvettes (1.00-cm pathlength) were purchased from Brookhaven Instruments. Sartorius brand Minisart® syringe filters (0.7 μm) were obtained from Fisher Scientific. Liquid Nitrogen was provided by Chemistry Department, Missouri State University.

2.2 Instrumentation

A Brinkmann PC-700 probe colorimeter was used to directly measure or read transmittance of a test solution in determining the cloud-point temperatures of PVCL-PVOH-PEG. A Vernier labquest® 2 model LQ2-LE and a Vernier temperature probe were used to collect data from the colorimeter. Flexi-Dry model-FD-3-85 lyophilizer was used to freeze dry the hydrolyzed Soluplus® solution.

Nanoparticle sizes and distributions were analyzed using dynamic light scattering (DLS). A Brookhaven Nanobrook Omni instrument utilizing a scattering angle of 90° and wavelength of 640.0 nm. For further characterization of size distributions, nanoparticle

tracking analysis (NTA) was performed by using Malvern instruments Ltd, Nanosight instrument with a model LM10 laser module.

The hydrolyzed Soluplus® product (PVCL-PVOH-PEG) was confirmed by ^{1}H NMR spectroscopy (Varian 400 MHz unit INOVA) using DMSO-d_6 as solvent and tetramethylsilane (TMS) as an internal chemical shift standard. Product confirmation also came from Fourier-transform infrared (FT-IR) spectroscopy (Bruker Vertex 70), in which samples were suspended in KBr pellets pressed at 9 tons of pressure by a Carver hydraulic press (model C).

2.3 Procedure

Hydrolysis of Soluplus®. In a 200 mL Erlenmeyer flask, 4 g of Soluplus® (PVCL-PVAc-PEG) was mixed with a solution of potassium hydroxide (0.8 g) in 150 mL of methanol and was stirred using a magnetic stirrer at room temperature for 18 hours. About 80% of the methanol was removed under reduced pressure and the PVCL-PVOH-PEG residual solution was diluted with about 5 mL of distilled water. The diluted solution was transferred to a dialysis tube and dialyzed through pore membrane with cut-off 500-1000 Da for 24 hours. The dialyzed aqueous solution was frozen using liquid nitrogen and lyophilized for 20 to 24 hours depending on the quantity of the sample. This was done in order to recover the copolymer product. The synthetic scheme is shown in Figure 5.

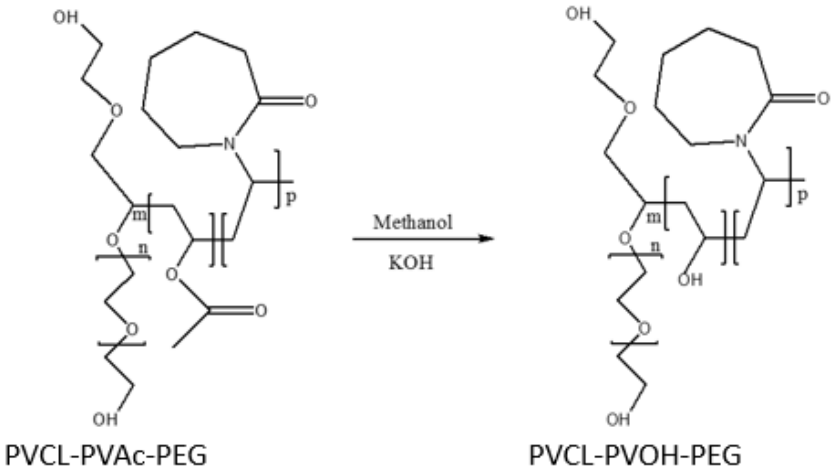

Figure 5 The hydrolysis of Soluplus® to PVCL-PVOH-PEG in Methanol and Potassium hydroxide at room temperature.

Cloud Point Determination. Cloud point temperatures were determined using a Brinkmann probe colorimeter and a Vernier LabQuest 2 data recorder. As the name implies, cloud point is the temperature at which the solution phase separates and becomes cloudy. A sample tube was placed in a water bath on a Corning PC-420D hotplate/ stirrer. The temperature probe (attached to the LabQuest) and photodiode (attached to the colorimeter) were inserted into the sample solution, and the temperature was raised at a rate of 0.02 $^{\circ}$C/ 2 seconds. The colorimeter was used to monitor light transmittance as the temperature increased. The labQuest recorded input from both the temperature probe and the DC voltage output of the colorimeter to record the transmittance and temperature of the solution every 2 seconds. An ice-bath was used for the cooling stage. The setup is depicted in Figure 6.

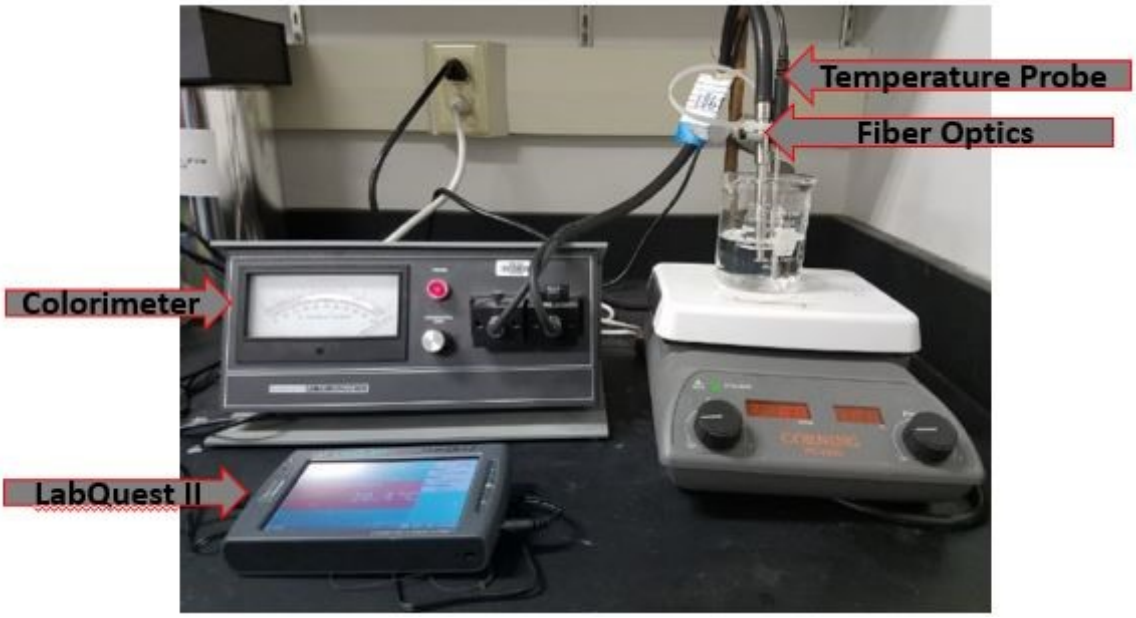

Figure 6. Cloud point measurement set up.

Different concentration (w/w) of PVCL-PVOH-PEG in aqueous solution were prepared ranging from 0.5% to 40%. The cloud point was determined and each measurement was repeated at least three times to determine statistical uncertainties. Data obtained from the LabQuest was imported into an excel spreadsheet where a plot of transmittance reading *vs* temperature (turbidity curve) was made for all solution concentrations. Figure 7 shows a representative result for cloud point determination of a 9% (w/w) PVCL-PVOH-PEG solution. To determine the cloud point, the best fit line as the value of transmittance tends to go to zero was determined (*i.e.*, inflection point).[50]

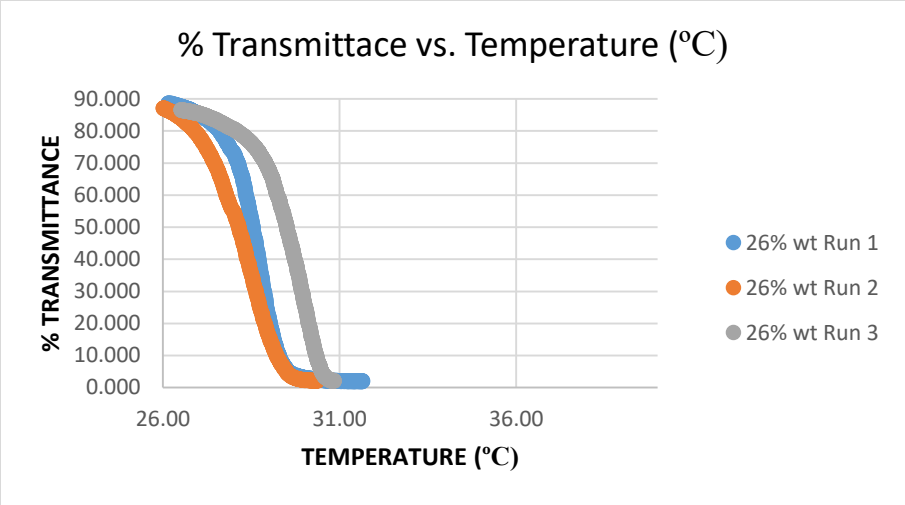

Figure 7. Representative result of cloud point measurement: A plot of transmittance reading *vs* temperature (˚C) of 26 (w/w) PVCL-PVOH-PEG solution.

Gel Point Measurement. To determine gel point of a given concentration, a sample tube with 4 mL of sample solution was placed in a 250 mL beaker containing water. The beaker and sample solution were placed on a hot plate with a lab stand, and a temperature probe was inserted into the sample and held by a lab stand clamp. The temperature probe was connected to a Vernier LabQuest used for reading the temperature of the solution. As the temperature of the sample solution increased, the solution turned cloudy. With further increase in temperature, the solution gelled. To determine the gel point, the test tube was turned 90˚ to check for flow as shown in Figure 8. The average temperature at which this process occurred was noted (gel point). The process is repeated at least twice to ensure reproducibility. Different concentrations of PVCL-PVOH-PEG in aqueous solution ranging from 5% - 60% (w/w) at 2.5% increments were prepared and each was analyzed using same procedure.

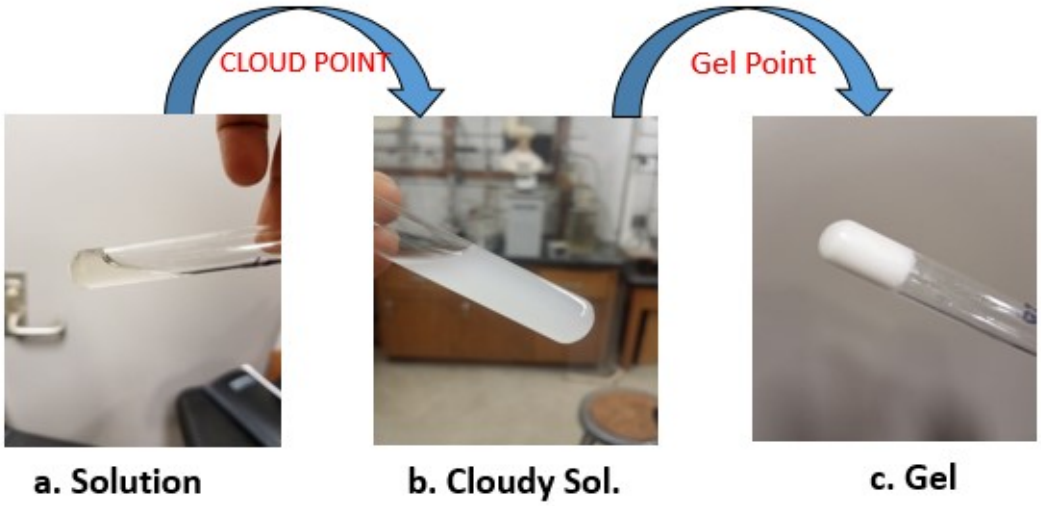

Figure 8: Gel point measurement: a) Sample in aqueous solution. b) Sample solution at cloudy point. c) Sample at gel point.

Particle Size and Distribution from DLS. The particle size distributions of PVCL-PVOH-PEG copolymer in water were determined by dynamic light scattering (DLS). Concentrations of 0.5% - 20% (w/w) were prepared by dissolving the sample into deionized water for 24 hours at room temperature to make sure it completely dissolved. The sample solution was filtered with a 0.7 µm Minisart syringe filter (rinsed prior to use) into a cuvette to help remove any dust or particle that might be present. The intensity of the scattered light was detected at an angle of 90°. Data were analyzed using an automatically calculated range selection, 640 nm wavelength and dust cut-off of 10. Each concentration was analyzed at 3 different temperatures, 25 °C (temperature below cloud point), 27 °C (cloud point temperature) and 30 °C (temperature above cloud point). A total of at least 5 runs were carried out for each temperature, 100 s/run at an equilibrium time of 10 seconds between runs.

Particle Size and Distribution from Nanosight. The instrument was cleaned by removing the power cord from the laser module and the four screw holding the top plate in place (see Figure 9). The optical flat was carefully removed from the top plate and rinsed with water and ethanol, wiped with tissue then allowed to dry. The same was done for the lower port and the glass surface of the top plate. Clean wash liquid (DI water) was injected into the chamber to ensure that there is no sample after cleaning before injecting PVCL-PVOH-PEG copolymer aqueous solution. A 1.00-mL syringe was used to load the sample, making sure that there was no air bubble in the sample syringe. The sample was injected into the lower port in the top-plate. Slowly the top-plate cell was filled, keeping the syringe in place. The laser module was placed on the microscope stage, and a temperature probe was attached to the laser module to keep track of the sample's temperature. The stage and focus was adjusted to a correct position and made ready for a measurement. A camera was synchronized with the laser module, and Nanosight NTA software (Ver. 2.3) was used to count the number and concentration of each particle size.

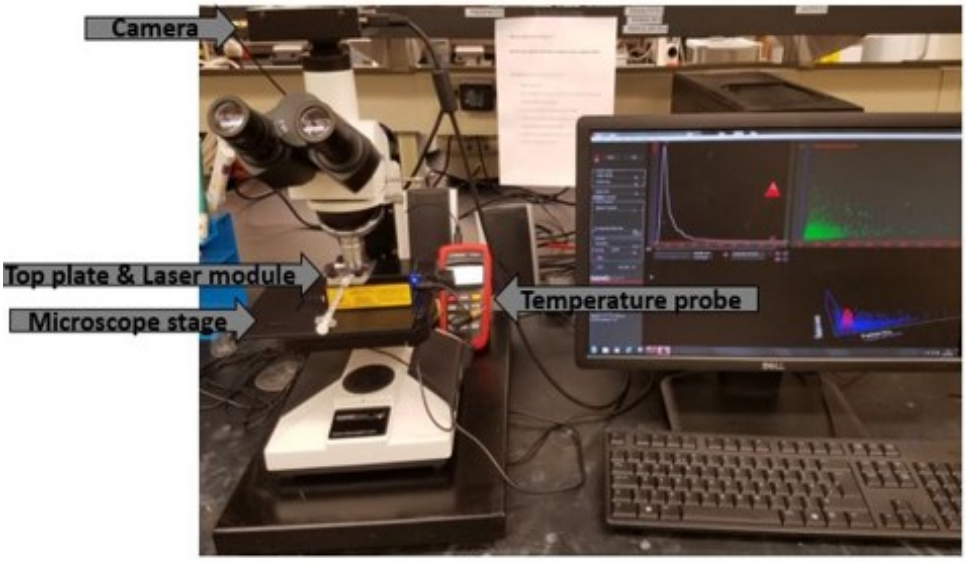

Figure 9: Nanosight instrument set up.

3. RESULTS AND DISCUSSION

3.1 Proton NMR and Infrared Spectroscopy

The hydrolysis of polymeric compounds containing an ester group is one of the oldest chemical process developed to obtain polymeric compounds with a hydroxyl group.[47,51,52] Polyvinyl acetate (PVAc) undergoes hydrolysis under mild conditions to yield polyvinyl alcohol (PVOH), a water soluble polymer. Soluplus®, the amphiphilic block graft copolymers, PVCL-PVAc-PEG, is therefore a suitable precursor for making triple hydrophilic block copolymer, PVCL-PVOH-PEG. Figure 10 shows the Proton NMR spectra of Soluplus® before and after hydrolysis recorded in DMSO-d_6.

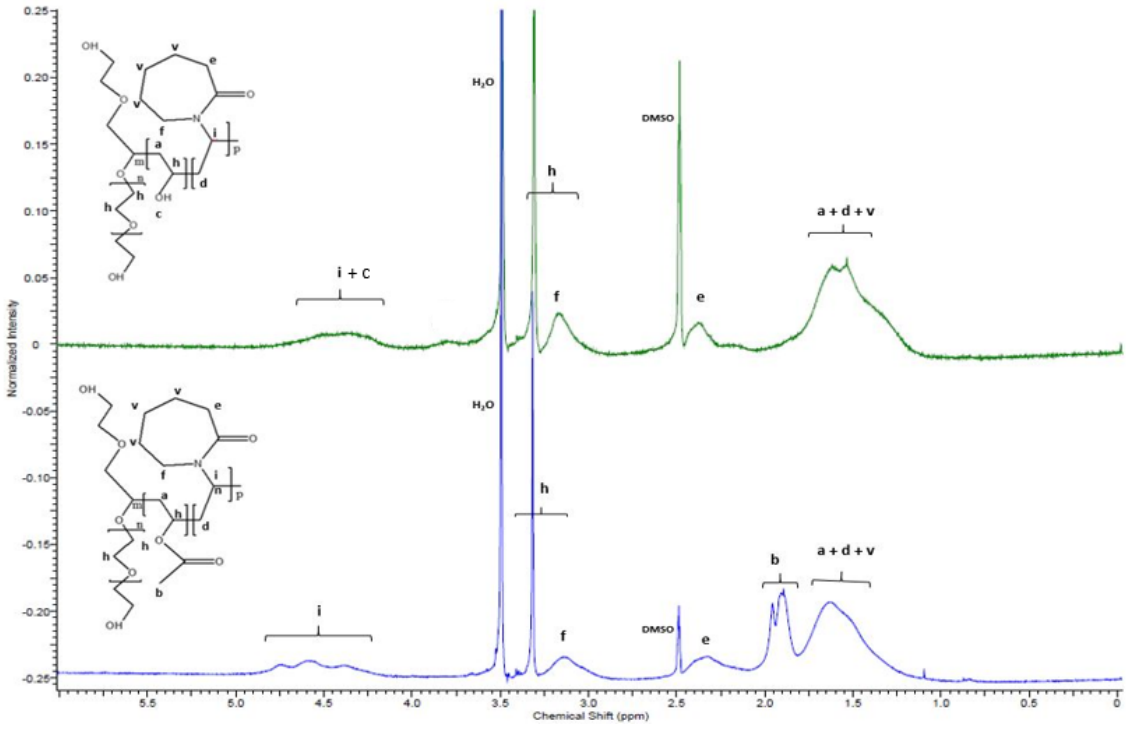

Figure 10. ^{1}H NMR spectra of Soluplus® before and after hydrolysis recorded in DMSO-d_6 at room temperature.

The hydrolysis of Soluplus® was carried out as described in Section 2.3.1. Proton NMR and IR spectroscopies were used to confirm the formation PCL-PVOH-PEG after the chemical process was complete. Resonances peaks (Figure 10) were processed using ACD/Labs (Advanced Chemistry Department Inc.) software. The spectra evidenced success of the process by the disappearance of the signal associated with the acetyl group of PVAc (Resonance b at 1.90 ppm) and the appearance of the hydroxyl group signal associated with of PVOH (Resonance c at 3.80 ppm), while the characteristic signals of PVCL and PEG remained the same in both spectra.

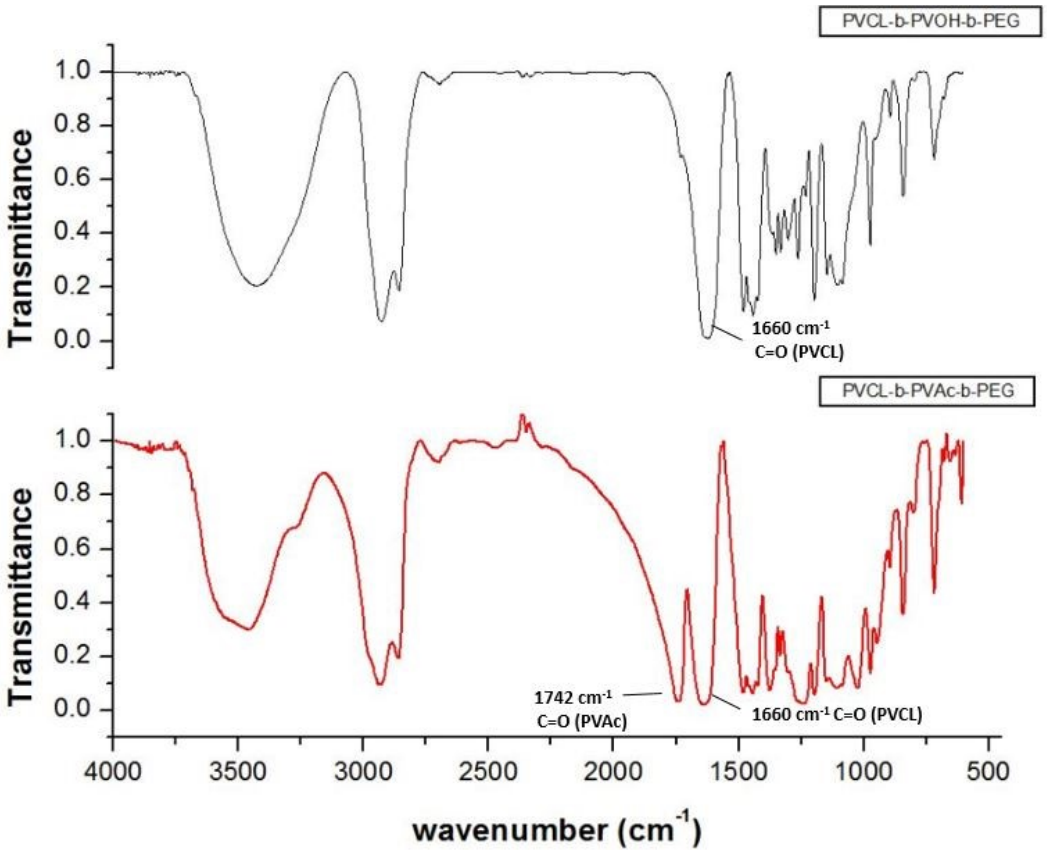

Figure 11. Infrared spectra of Soluplus® before and after hydrolysis, recorded in KBr pellet pressed at 9 tons pressure by a carver hydraulic press.

Similarly, the infrared spectra evidenced hydrolysis success by the disappearance of the absorption band associated with the carbonyl stretching mode (C=O) of PVAc at 1742 cm^{-1}, while the absorption band associated with carbonyl stretch of PVCL at 1660 cm^{-1} and the C-N stretch at 1490 cm^{-1} remained the same for both spectra. Together, the proton NMR and IR data confirm the complete hydrolysis of Soluplus® to PVCL-PVOH-PEG. The infrared spectra is shown in Figure 11. The ^{1}H NMR and IR spectra reported here are similar to that of PVAc-PVCL and PVOH-PVCL reported by Hurtgen, *et al*.[47]

3.2 Molecular weight distribution

According to BASF technical information sheets, the molecular weight of Soluplus® was determined by gel permeation chromatography (GPC) using poly(methyl methacrylate) as a reference. The average mass was reported to be in the range of 90,000 to 140,000 g/mol, with an average molar mass of 118,000g/mol (Figure 12).[44]

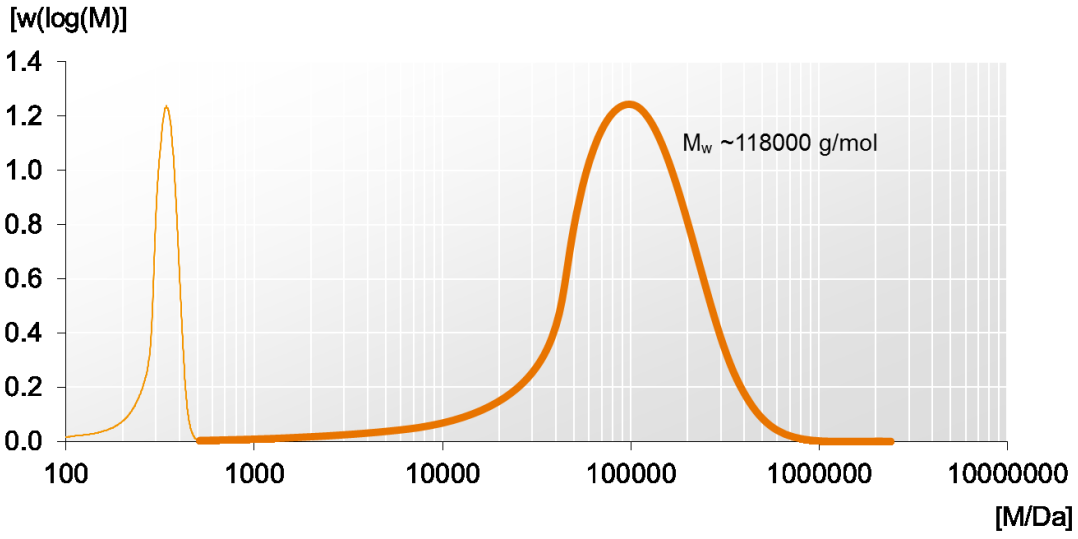

Figure 12 The molecular weight distribution of Soluplus®.[44]

Here we report the MALDI mass spectrum of Soluplus® measured at Pittsburg State University as shown in Figure 13. The most intense peak (A) in the spectrum at *m/z* = 102,507 was assumed to be the molecular ion. The peaks on this spectrum are few and appeared as sharp peaks which are unusual and quite different from the broader peaks expected and observed in large synthetic polymer MALDI spectra.[53,54,55] This makes it difficult to evaluate the ionization process. However, the MALDI molar mass is consistent with the GPC data reported by BASF.

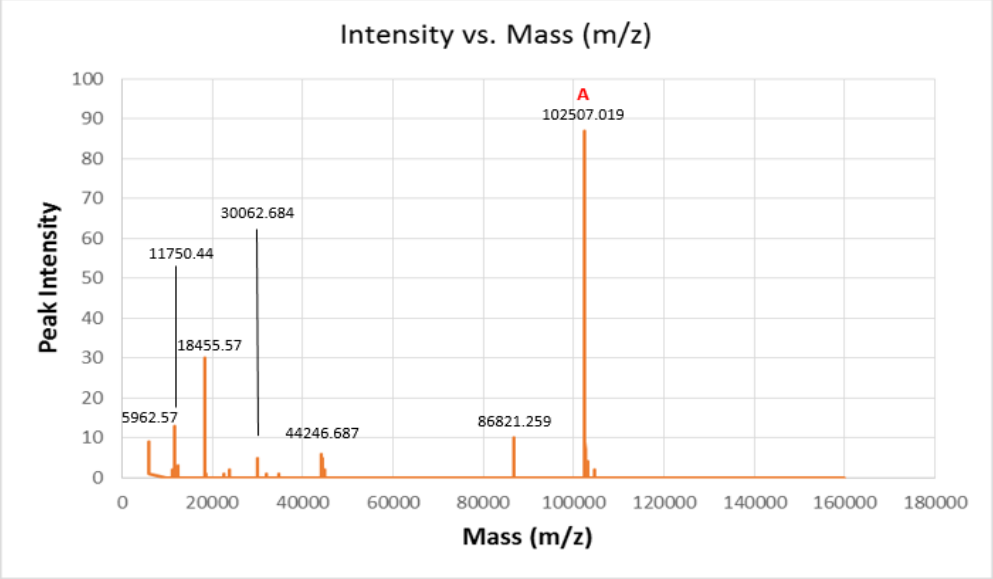

Figure 13. MALDI-TOF mass spectrum of Soluplus®.

3.3 PVCL-PVOH-PEG Number-Average Molecular Weight Calculation. The expected *Mn* value for the PVCL-PVOH-PEG was calculated as follows;

The molecular weight of 1 repeating unit: PVCL ($C_8H_{13}N0$) = 139.19 g/mol

PVAc ($C_4H_60_2$) = 86.09 g/mol

PEG (C_2H_4O) = 44. 05 g/mol

PVOH (C_2H_4O) = 44. 05 g/mol

Based on the mole ratio in Soluplus®, a "formula mass" can be determined as:

PEG (13%): PVAc (30%): PVCL (57%) = (44.05 × 13) + (86.09 × 30) + (139.19 × 57)

= 11,089

Based on the presumed complete conversion from Soluplus®, the formula mass of the hydrolyzed products is:

PEG (13%): PVOH (30%): PVCL (57%) = (44.05 × 13) + (44.05 × 30) + (139.19 × 57)

= 9828

Therefore the number of "formula units" in Soluplus® = 102,507 ÷ 11.089 = ~9 units, and the expected Mn of PVCL-PVOH-PEG = 9 × 9828 = ~88,452 g/mol.

From the mass evaluation of Soluplus® directly above, the expected mass of PVCL-PVOH-PEG was calculated to be 88,452 g/mol. Figure 14 shows the MALDI mass spectrum of PVCL-PVOH-PEG.

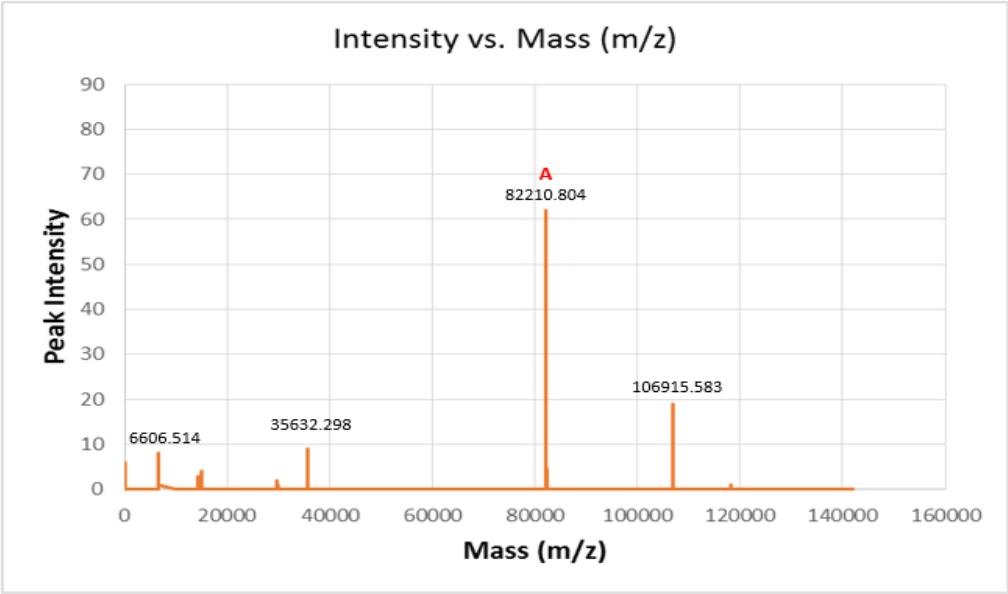

Figure 14. MALDI-TOF mass spectrum of PVCL-PVOH-PEG.

With this, the molecular ion in the MALDI spectrum of PVCL-PVOH-PEG (Figure 14) was assumed to be the peak A (the most intense peak with *m/z* = 82,210), since it is the closest mass to the expected value. Again the peaks in this spectrum are similar to those observed in Soluplus® MADLI spectrum. This may be as a result of experimental parameters such as number of laser shot, the relative proportion of polymer and the nature of the matrix used.

3.4 Cloud Point Data

The phase and conformational behavior of Soluplus® as a function of temperature and concentration obtained from previous study by Balzam[50] has been reproduced here in Table 4 and Figure 15 for comparison purposes. As can be seen in the data, the cloud point varies with concentration of Soluplus®.

Table 4. Cloud point result: cloud point and SD for each Soluplus® concentration.

%Wt	*T* (˚C)	SD* (˚C)	%Wt	*T* (˚C)	SD* (˚C)
0.5	29.9	0.5	16	28.2	0.1
1	30.9	0.3	17	27.7	0.3
2	30.4	0.2	18	28.4	0.4
2.5	30.8	0.4	19	28.6	0.3
3	30.6	0.7	20	28.0	0.2
4	29.5	0.2	21	28.6	0.2
5	29.4	0.1	22	28.4	0.8
6	28.7	0.1	23	29.3	0.4
7	28.4	0.1	24	28.8	0.3
8	27.6	0.4	25	28.6	0.3
9	27.0	0.3	26	29.0	0.1
10	26.7	0.4	27	29.2	0.1
11	27.0	0.1	28	30.2	0.1
12	27.2	0.2	29	30.7	0.2
13	28.2	0.3	30	28.8	0.1
14	28.3	0.5	35	29.4	0.4
15	27.6	0.2	40	30.9	0.2

*SD represents standard deviation (n = 3)

The results from this study showed that cloud point decreased with increasing Soluplus® concentration from 1% to10% (w/w) and then increased as the concentration continued to rise from 11% to 30% (w/w), exhibiting a lower critical solution temperature (LCST) of 26.7 ˚C at 10% concentration. This behavior is similar to the phase transition behavior of PVCL in water in which the cloud point shift to a lower temperature when polymer chain length increases.[56,57,58] Experimental cloud point measurements and theoretical calculations have been carried out by Meada, *et al*, and it was concluded that the phase behavior of PVCL in water represents Flory- Huggins miscibility behavior (Type 1).[56]

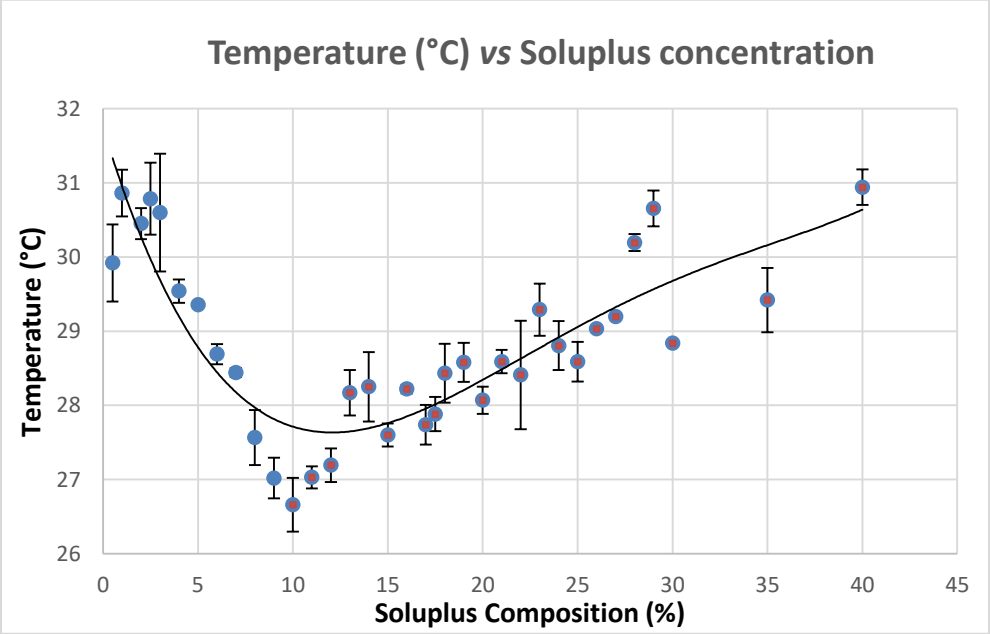

Figure 15. Lower critical solution temperature curve of Soluplus®: plot of the overall cloud point versus their corresponding concentrations.[50]

Unlike Soluplus®, PVCL-PVOH-PEG block copolymers are expected to be more hydrophilic at room temperature and becomes amphiphilic upon heating. This behavior is

based on the fact that PVCL undergoes heat induced phase transition in water (monomer with amphiphilic properties), owing to the dehydration of PVCL chain.[47]

Table 5 presents cloud point data for PVCL-PVOH-PEG. The result shows that the cloud point decreases with increasing PVCL-PVOH-PEG concentration from 0.5% to 5% (w/w) and increased from 7% to 14% (w/w), exhibiting a lower critical solution temperature (LCST) of 26.8 ºC similar to that of Soluplus® at 6% concentration. Above 14% concentration, the cloud point temperature vary weakly and stay in the range of 27˚C to 28 ˚C, which is lower than observed for Soluplus®.

A similar result to this observation was reported by Yanul, *et al*,[59] for a Poly(N-vinyl caprolactam)-Poly(ethylene oxide) (PVCL-PEO) system, where the introduction of hydrophilic PEO into the aqueous solution of PVCL weakens the strength of hydrogen bonds in the PVCL-water system and thereby causing a decrease it's phase transition temperature. On the other hand, the observed behavior is different to that observed for PNIPAM-based thermoresponsive copolymer, in which the increase in hydrophilic groups or chains lowers cloud point temperature.[46,47,48,49] This contrast strongly suggest that the effect of hydrophobic or hydrophilic balance on cloud point temperature in thermoresponsive polymer systems is a complicated phenomenon, regulated by many interconnected factors.[59] In the case of this study it can apparently be influenced by the solution behavior of PVOH, its interactions with other blocks (PVCL, PEG) and perhaps also to the degree of hydrolysis.

Table 5. Cloud point result: showing the cloud point and standard deviation for each PVCL-PVOH-PEG tri-block copolymer concentration.

%Wt	*T* (˚C)	SD* (˚C)	%Wt	*T* (˚C)	SD* (˚C)
0.5	27.75	0.48	17	28.39	0.47
1	27.81	0.36	18	27.59	0.04
2	27.02	0.28	19	28.49	0.04
3	27.54	0.42	20	27.68	0.23
4	26.94	0.42	21	28.39	0.12
5	27.17	0.05	22	28.18	0.28
6	26.84	0.02	23	28.54	0.20
7	27.54	0.12	24	28.15	0.15
8	27.54	0.11	25	28.73	0.33
9	27.58	0.09	26	28.84	0.85
10	27.81	0.16	27	28.10	0.67
11	27.64	0.26	28	28.78	0.50
12	27.82	0.26	29	28.83	0.64
13	28.08	0.07	30	28.22	0.93
14	28.32	0.64	35	28.14	0.95
15	28.20	0.20	40	28.22	0.65
16	27.36	0.22			

*SD represents standard deviation (n = 3)

Figure 16 shows the cloud point curve of PVCL-PVOH-PEG over the concentration range of 0.5% to 40% (w/w). The graph shows transition temperatures ranging from 26˚C to 28˚C for all the polymer concentration measured.

A curve showing the lower boundary of the phase diagram, where the critical point shifts towards the lower concentrations as the concentration of the polymer solution increases (Figure 17) was observed from 0.5% to 14% (w/w). This may also suggest that the strength of the hydrogen bonds within the Soluplus®-water system is weakened by the introduction of hydrophilic PVOH which also interact with water.[59]

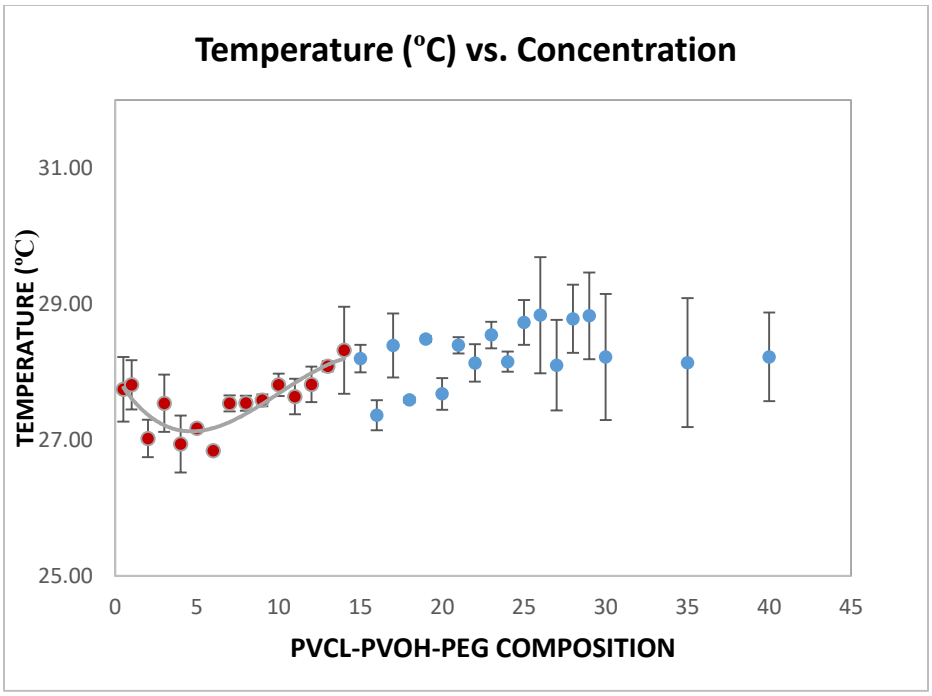

Figure 16. Lower critical solution temperature curve of PVCL-PVOH-PEG copolymers: plot of the overall cloud point versus their corresponding concentrations.

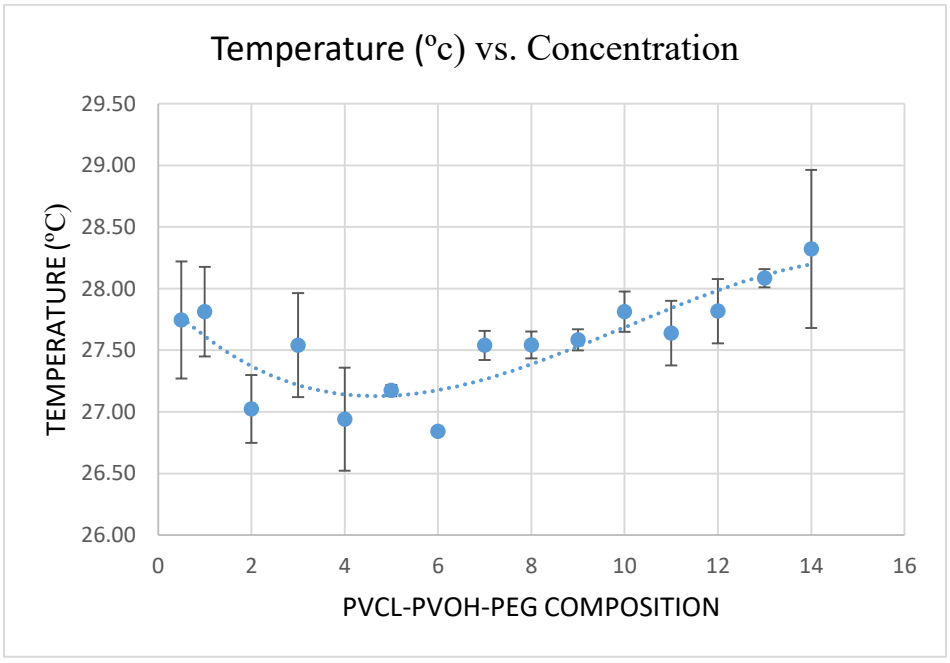

Figure 17 Lower critical solution temperature curve of PVCL-PVOH-PEG copolymers of 0.5% to 14% concentration.

3.5 Gel Point.

Sol-gel transition temperatures for Soluplus® in aqueous solution were determined by the test tube tilting method.[60] The range of the concentrations measured was 5%-30%, and the temperature at which the gel become solution again (gel-sol transition temperature) was measurable over a concentration range 12.5% to 17%. The results are presented in Table 6. These data show that Soluplus® solution did not gel at concentrations below 10% and at concentrations above 30% the solutions were effectively gelled at room temperature.

The Soluplus® sol-gel phase diagram, Figure 18, is similar to that observed for a PEG-based copolymer based on poly(ethylene glycol-*b*-[lactic acid-*co*-glycolic]-*b*-ethylene glycol) (PEG-PLGA-PEG),[61] reproduced in Figure 19.

Table 6. Gel point results: Average gel points and standard deviation for each Soluplus® concentration.

Conc. %Wt	Avg. Temp. (ºC)	SD* (ºC)	Avg. USGT (ºC)	SD* (ºC)
5	N/A	N/A		
7.5	N/A	N/A		
10	53.7	1.15		
12.5	45.7	2.29	60.3	1.5
15.0	42.9	1.44	63.8	1.0
17.5	40.1	1.22	68.5	0.5
20	39.6	1.15		
22.5	38.3	0.38		
25	33.5	0.12		
27.5	32.9	0.06		
30	30.5	0.14		

*SD represents standard deviation (n = 3)

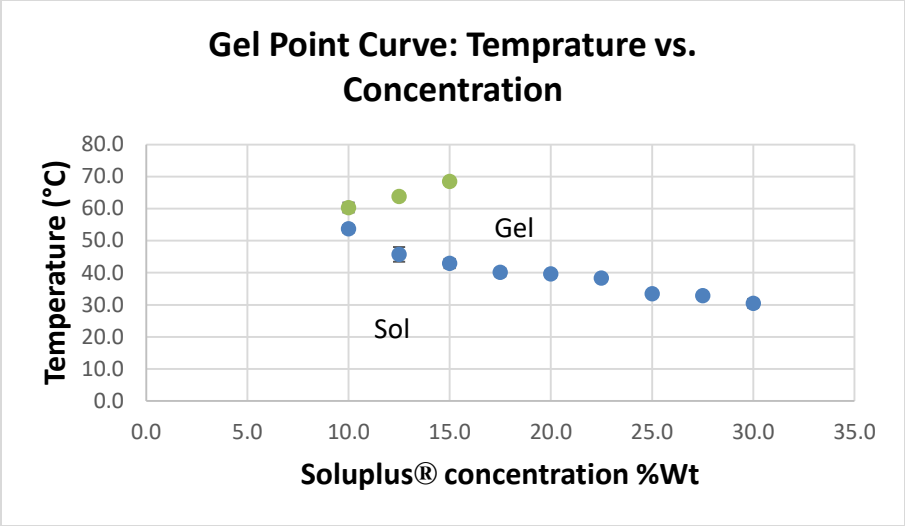

Figure 18. Sol-gel transition curve of Soluplus® determined by test tube tilting method: plot of overall average gel points versus polymer concentration. The green data points represents the upper sol-gel transition temperature. Error bars represent ±1.0 standard deviations as determined by multiple, independent measurements.

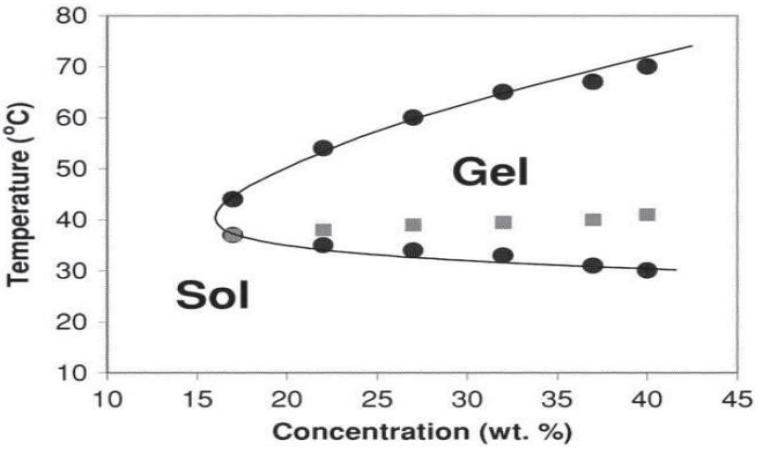

Figure 19. Gel point curve of aqueous solutions of the tri-block copolymer, poly(ethylene glycol-*b*-[lactic acid-*co*-glycolic]-*b*-ethylene glycol) (PEG-PLGA-PEG), in aqueous solution (reproduced from Ref. 57).

The sol-gel transition behavior of PVCL-PVOH-PEG copolymers was also determined by test tube tilting method, the data from this study is presented in Table 7 and Figure 20. Concentrations in the range of 5%-60% were analyzed. Unlike for Soluplus®, we were unable to observe gel-sol transition for PVCL-PVOH-PEG at higher

temperatures due to the already high temperatures needed to induce sol-gel transitions and the limited temperature range afforded by the water bath. Sol-gel transitions were observed for concentrations 25% to 60% (w/w). Solutions with concentrations below 25% did not gel. Generally, the sol-gel transition curve of PVCL-PVOH-PEG in solution is similar to that of Soluplus® but is shifted both to higher temperature and to higher concentration. This is consistent with previous reports that increasing hydrophilic content in thermoresponsive polymer solutions tends to shift the phase boundaries in these ways [49,62,63,64,65] Such behavior suggests that that hydrophobic interactions are the key mechanism of the thermogelation process in PEG-based copolymers, including Soluplus® and its hydrolyzed analog.

Table 7. Gel point results: Average gel points and standard deviation for each PVCL-PVOH-PEG copolymers concentration.

Conc. %w	Avg. Temp. (˚C)	SD* (˚C)
5	N/A	N/A
10	N/A	N/A
15	N/A	N/A
20	N/A	N/A
25	88.4	0.49
27.5	85.0	0.00
30	81.5	0.71
32.5	81.5	0.21
35	80.8	1.06
37.5	78.6	0.57
40	76.9	0.21
42.5	73.3	0.35
45	67.7	0.49
47.5	67.1	0.14
50	63.2	1.13
52.5	63.7	0.42
55	62.5	0.71
57.5	60.5	0.64
60	58.6	0.85

*SD represents standard deviation

In principle, polymers with amphiphilic properties physically cross link via reverse thermogelation, as temperature is increased[19] as seen in Figure 2. The hydrophobic segment (sometimes called the gelator) aggregates to minimize its contact with water, and maximizing the solvent entropy. The more hydrophobic the block, the larger the entropy cost of water structuring, and the larger the driving force for hydrophobic aggregation. Thus, the sol-gel transition temperature shifts to lower temperature.[19] However, when the hydrophilicity effect overwhelms the entanglement effect or aggregation effect, the sol-gel transition temperature increases,[63] which is what was observed for the thermal gelation process in the PVCL-PVOH-PEG copolymer.

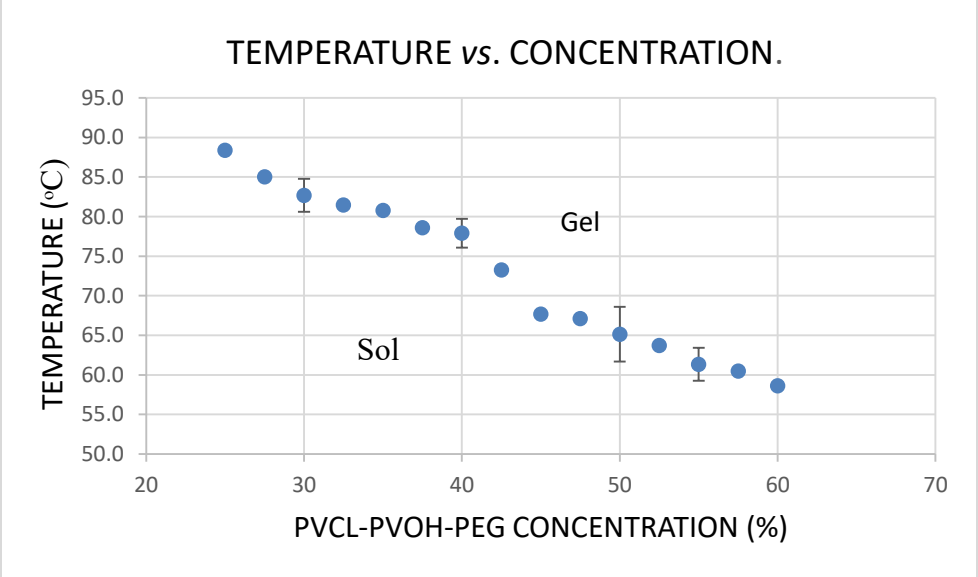

Figure 20. Sol-gel transition curve of PVCL-PVOH-PEG aqueous solutions determined by test tube inverting method: plot of overall average gel points versus polymer concentration.

3.6 Particle Size and Distribution.

Soluplus® is expected to be amphiphilic at room temperature and become more hydrophobic at temperature above cloud point temperature of their aqueous solutions, owing to the dehydration of PVCL sequence.[47] The DLS result in Table 8 shows that Soluplus® forms micelles in water at room temperature, and expectedly, the sizes increases as a result of aggregation from individual polymeric micelles as the temperature was raised above their cloud temperatures. Concentrations between the range of 4% to 20% were measured at temperatures below cloud point (room temperature), at cloud point, and temperatures above cloud point. As expected, the sizes of the particles for each of the concentrations increased at temperature above their cloud point.

Data from Table 8 also show that micelle size increases down the table, which is with increase in polymer concentration. It was also observed that the polydispersity distribution of the micelles at lower polymer concentrations and lower temperatures are narrower compared to higher polymer concentrations and temperatures. Figure 21 show a lognormal size distribution graph for 4% w/w Soluplus® solution at various temperatures.

PVCL-PVOH-PEG copolymer are expected to be hydrophilic at room temperature, again owing to the dehydration of PVCL sequence,[47] It should become amphiphilic at temperature above its cloud point, and it is expected to self-assemble with PVCL sequence as the core and soluble PVOH-PEG segments as the corona (shell).

Table 8. Summary of DLS data of Soluplus®and corresponding PVCL-PVOH-PEG in water

PVCL-PVOH-PEG				**SOLUPLUS**			
Conc. (%wt)	*T* (˚C)	D_h (nm)	PDI*	Conc. (%wt)	*T* (˚C)	D_h(nm)	PDI*
4%	25	160	0.40	4%	25	73	0.04
	27	134	0.38		27	74	0.11
	30	1,733	0.27		30	75	0.09
					35	174	0.30
8%	25	187	0.37	8%	25	74	0.08
	27	166	0.34		27	83	0.13
	30	1,789	0.19		30	75	0.08
					35	176	0.31
12%	25	215	0.38	12%	25	131	0.28
	27	191	0.34		27	115	0.22
	30	2,413	0.31		30	106	0.21
					35	457	0.40
16%	25	154	0.36	16%	25	191	0.31
	27	316	0.37		27	169	0.29
	30	1,883	0.24		30	135	0.26
					35	992	0.44
18%	25	249	0.37	20%	25	407	0.35
	27	306	0.36		27	352	0.37
	30	989	0.35		30	232	0.32
					35	4,299	0.47

*Polydispersity (PDI)

However, we observed that PVCL-PVOH-PEG copolymers self-assemble at room temperature, and they increased further in size at temperatures above the cloud point (Figure 22). The polydispersity becomes more moderate compared to that of Soluplus®, as well. A Summary of the data obtained from DLS measurements are presented in Table 8. Figure 23 also show that the increase in size of the PVCL-PVOH-PEG aggregates

depends on time at temperatures above cloud point. A 12% concentration was investigated at 30˚C.

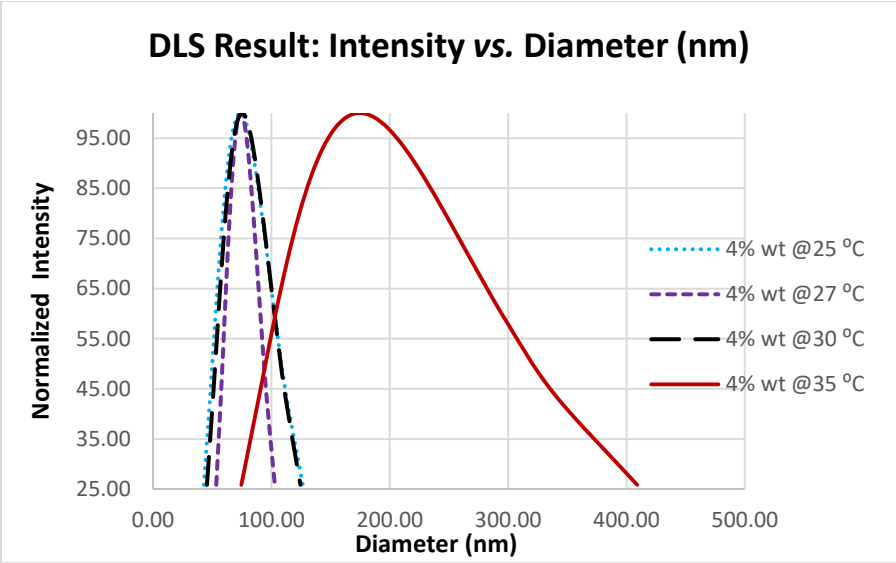

Figure 21. Size distribution graph of Soluplus® micelles in water at various temperatures: 4% w/w at 25 ˚C, 27 ˚C, 30 ˚C and 35 ˚C.

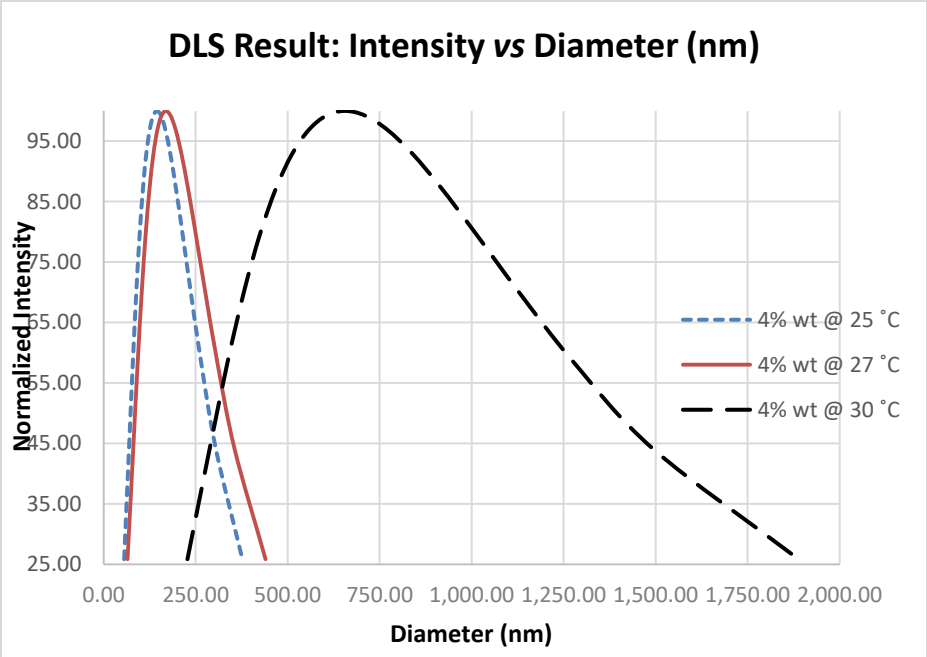

Figure 22. Size distribution of PEG-PVOH-PVCL coplymer micelles in water at various temperatures: 4% w/w composition analyzed at 25 ˚C, 27 ˚C, 30 ˚C and 30.5 ˚C.

The temperature was kept constant, but the number of runs was increased to three. The timeframe for each run was 100 seconds with a resting time of 10 seconds between the three runs. Over the course of the three runs, the particle size increased from 311 nm (Run 1) to 2,455 nm (Run 3).

Generally, the sizes of Soluplus® micelles at lower concentrations (4%, 8% and 12%) are significantly smaller than micelles of PVCL-PVOH-PEG copolymers in this same concentration range. This suggest that a more hydrophobic sequence results in a more stable, and closely packed micelles.[6] The formation of micelles by PVCL-PVOH-PEG copolymers at room temperature is unusual, which suggest that PVCL block exhibit amphiphilic properties even at room temperature-that is, a hydrophilic segment (carboxylic and amide groups) and hydrophobic segment (carbon-carbon backbone).

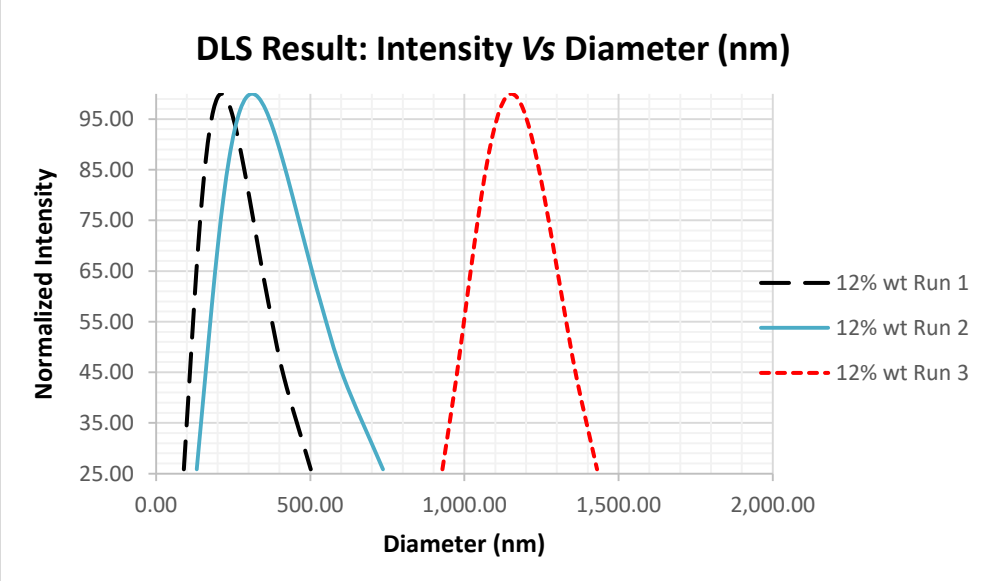

Figure 23. Size distribution of PVCL-PVOH-PEG micelles in water at a constant temperature over time: 12% w/w composition analyzed at 30 ˚C over time (300s).

To corroborate the size distribution obtained from DLS and to enable a thorough size distribution analysis of PVCL-PVOH-PEG copolymers at room temperature, nanoparticle tracking analysis (NTA) measurements were performed using a Malvern NanoSight instrument to confirm the sizing data obtained from DLS. For the NTA measurement, 15% and 10% (w/w) concentration samples of PVCL-PVOH-PEG copolymers in water were prepared according to the procedure stated in Section 2.3.5. The samples were analyzed at 22 ˚C. One of the disadvantages of the Nanosight instrument is that it does not have a heating block enabling a live monitoring of the particles at controlled temperatures. Since NTA uses the Brownian motion of individual particle to calculate nanoparticle size, this method was used to count the number of particles and concentration of each particle size (Figure 24).

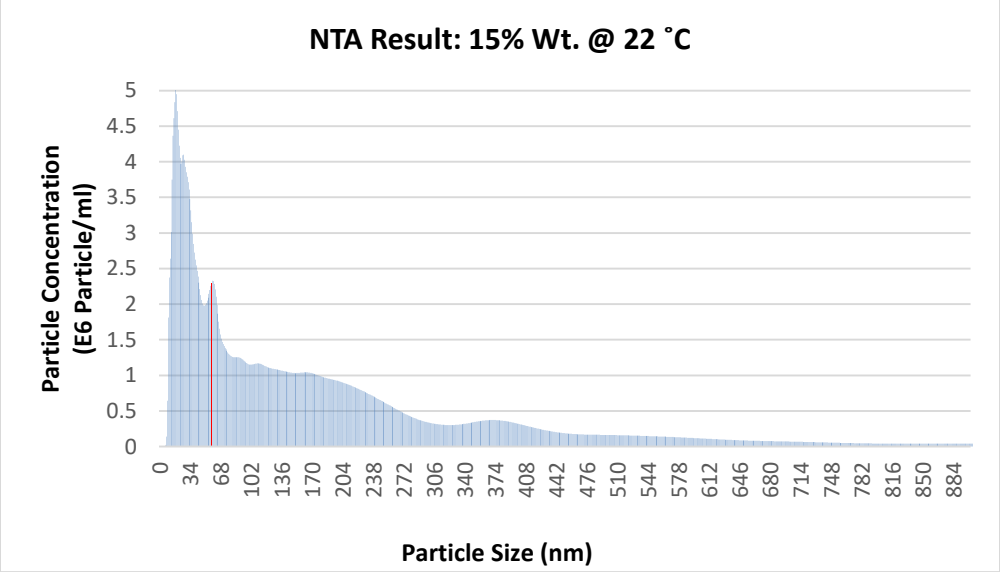

Figure 24. Size distribution of PVCL-PVOH-PEG copolymers (15% w/w) from NTA measurement: column chart of particle concentration, the number of particles within a given size range (10^6 particle/ml) versus particle size (nm) at 22 ˚C.

Upon collecting a total of 2265 completed tracks, a significant concentration of particles was observed at smaller diameters (30-66 nm). The mean of the size within the distribution was reported as 189 nm, with a standard deviation of 205 nm. The high standard deviation suggest that the sample has a very high polydispersity index. Figure 25 shows a typical video frame image from the Nanosight instrument for a 15% aqueous solution of PVCL-PVOH-PEG.

After 19909 completed tracks, a 10% (w/w) solution of PVCL-PVOH-PEG copolymers was analyzed by NTA at 22 ˚C. The resulting distribution is shown in Figure 26. A significant concentration was observed in the particle size range of 37 nm to 100 nm, with a mean value of 112$\pm$92 nm. Again, the large standard deviation suggests a rather high polydispersity index.

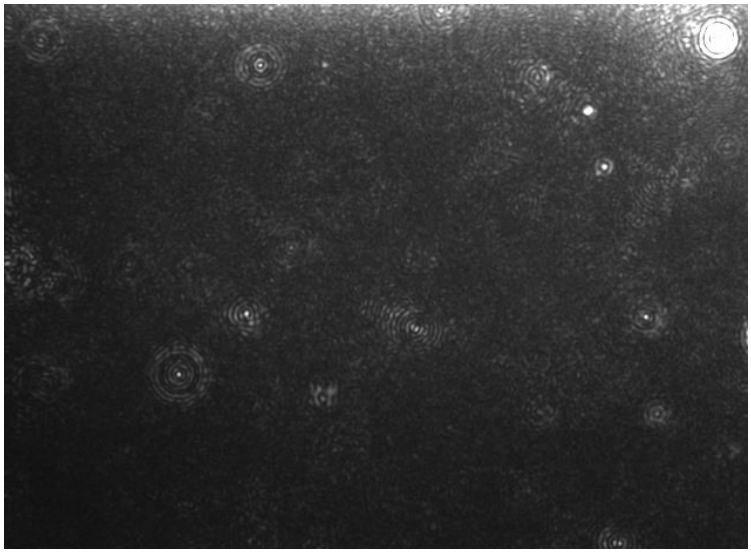

Figure 25. Size distribution of PVCL-PVOH-PEG (15% w/w.) copolymers from NTA measurement: corresponding video frame at 22 ˚C.

Generally, the NTA measurement at 22 ˚C provided insight to the number of particles present in a given size range and to visualize them. Both results from DLS and NTA imply that PVCL-PVOH-PEG copolymers self-assemble in water even at room temperature and subsequently suggest that the polymer still exhibits some level of hydrophobicity (not completely hydrophilic) in water at room temperature.

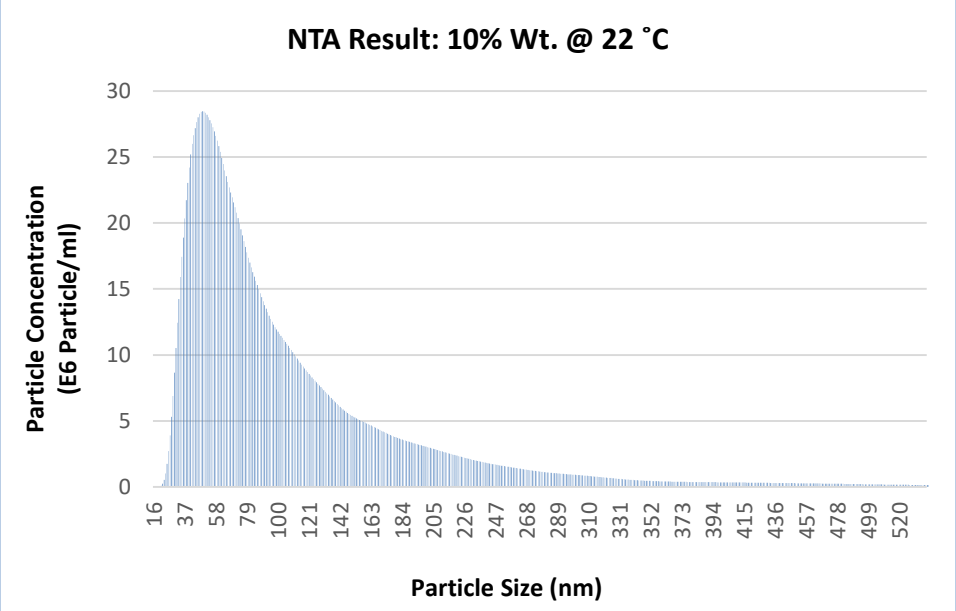

Figure 26. Size distribution of PVCL-PVOH-PEG copolymers (10% w/w) from NTA measurement: column chart of particle concentration, number of particle within a given size range (10^6 particle/ml) versus particle size (nm) at 22 ˚C.

4. CONCLUSIONS AND FUTURE WORK

4.1 Conclusions

Soluplus® a tri-block graft copolymers, was originally designed for preparing solid solutions of poorly water soluble drugs via hot melt extrusion technology, and studies have shown that Soluplus® increases the solubilities of several APIs in oral applications and topical creams and gels. However, to date, there is little information available about the physical and chemical properties of Soluplus®, though the thermoresponsive behavior in water (phase transition temperature and sol-gel transition temperature) has been studied and reported by Balzam.[50] The goal of this study was to hydrolyze Soluplus® and study its thermoresponsive behavior in water in comparison to the thermoresponsive behavior of Soluplus®.

According to BASF technical information sheet, the average molecular weight of Soluplus® determined by gel chromatography is in the range of 90,000-140,000 g/mol. The mass of Soluplus® (102,507) obtained from the MALDI-TOF mass spectrum was consistent with that obtained from BASF technical sheet. The mass of PVCL-PVOH-PEG (82210) from the MALDI-TOF mass spectrum was off compared to the expected value (88,451 g/mol).

The cloud point phase diagram of PVCL-PVOH-PEG exhibits similar behavior to that of Soluplus® from 0.5% to 14% (w/w) and has little to no dependence on polymer concentration from 14% upward. Overall, the cloud points were observed to occur at lower temperatures than those of Soluplus®. These observations are inconsistent with the

conventional theory that cloud point temperature increases with an increase in relative hydrophilicity of the polymer.

The sol-gel transition temperatures of PVCL-PVOH-PEG in solution were higher than those of Soluplus® solutions, and it is unclear if it exhibits an upper gel-sol transition temperature. These results are consistent with the trends that more hydrophobic the blocks leads to a larger entropy cost of water structuring which subsequently creates a larger driving force for hydrophobic aggregation, and a lower the sol-get transition temperature.

Particle-size distributions results from both DLS and NTA measuremnts shows that whereas Soluplus® particles increase with increase in polymer concentration, and larger aggregates are formed at temperatures above cloud point as expected, particles of PVCL-PVOH-PEG copolymers in solution behave more randomly. At lower concentrations the sizes of Soluplus® particles are smaller compared to those of PVCL-PVOH-PEG copolymers, which is attributed to the higher hydrophobicity of Soluplus®. PVCL-PVOH-PEG copolymers self-assemble even at room temperature which suggests that PVCL-PVOH-PEG copolymers are not completely hydrophilic in water.

Conclusively, the properties of thermoresponsive polymers can be manipulated by increasing or decreasing their hydrophilicity/hydrophobicity. In the case of this study, the conversion of PVAc to PVOH in Soluplus®, resulted into a more hydrophilic compound (PVCL-PVOH-PEG) with less physiological properties.

4.2 Future Work

The conclusions drawn from this project shows that the decrease and increase of phase transition temperature in theremoresponsive polymers based on PVCL has a lot to do with the interactions between each monomer unit and the solvent. In the case of this study, detailed investigations are needed to evaluate the complex thermoresponsive solution behavior of PVCL-PVOH-PEG copolymers by analyzing various degree of hydrolyzed Soluplus® (partial hydrolyzed analogs).

Future investigation can be carried out on both Soluplus® and PVCL-PVOH-PEG copolymers, by loading their micelles with hydrophobic drug molecules during the self-assembly process and analyzing them using DLS or NTA method at different temperatures to see what effect this will have on their sizes. As seen in literatures, the sizes of these micelles should increase upon loading and stabilize at a particular size range, suggesting a successful self-assembly process between the hydrophobic drug and the amphiphilic polymer.

Previous study by Balzam,[50] has shown that Soluplus® can increase the solubility and concentration of APIs in skin creams. The gel point phase diagram shows how soluble PVCL-PVOH-PEG copolymer is in water compared to Soluplus®. The study by Balzam may be reproduced using PVCL-PVOH-PEG, in order to evaluate its effect on the solubility of active pharmaceutical ingredients

5. REFERENCES

1. Ward, M. A.; Georgiou, T. K. *Polymers.* **2011**, *3*, 1215–1242.

2. Swanson, J. P.; Monteleone, L. R.; Haso, F.; Costanzo, P. J.; Liu, T.; Joy, A. *Macromolecules* **2015**, *48*, 3834–3842.

3. Jiang, S.; Yao, Y.; Chen, Q.; Chen, Y. *Macromolecules* **2013**, *46*, 9688–9697.

4. Bergbreiter, D.E.; Reagan, H; Jacqueline, B.; Chunmei, L.; Osburn, P. L. *J. Am. Chem. Soc*. **2003**, 125, 8244-8249.

5. Yasushi, M.; Tomoya, N.; Ikeda, I. *Marcromolecules* **2001,** 35, 217-222.

6. Gang-Biao, J.; Daping, Q.; Kairong, L.A.; Wang, H. *Mol. Pharm*. **2005**, 3, 152-160.

7. Durme, K.V.; Loozen, E.; Nies, E.A; Mele, B.V. *Macromolecules* **2005**, 38, 10234-10243.

8. Hou, X. (Engineer). *Design, fabrication, properties, and applications of smart and advanced materials*; CRS Press: New york, 2016; pp 1-489.

9. Ohm, C.; Brehmer, M.; Zentel, R. Adv. Polym. Sci. **2012**, 250, 49–93.

10. Aguilar, M. R.; Roman, J. S. *Smart polymers and their applications.*; Woodhead Publishing: Cambridge, 2014; pp 1-584.

11. Wei, P.; Cook, T. R.; Yan, X.; Huang, F.; Stang, P. J. *J. Am. Chem. Soc.* **2014**, *136*, 15497–15500.

12. Richards, G. J.; Labuta, J.; Hill, J. P.; Mori, T.; Ariga, K. *J. Phys. Chem. Lett.* **2010**, *1*, 1336–1340.

13. Qiu, X.P.; Tanaka, F.; Winnik, F.M. *Macromolecules* **2007**, 40, 7069-7071.

14. Zhang, Z. *Switchable and responsive surfaces and materials for biomedical applications;* Woodhead Publishing: Massachusett, 2014; pp 1-324.

15. Elliott, L. C. C.; Barhoum, M.; Harris, J. M.; Bohn, P. W. *Langmuir* **2011**, *27*, 11037–11043.

16. Qiu, Q.; Somasundaran, P.A; Pethica, B. A. *Langmuir* **2002**, 18, 3482-3486.

17. Gandhi, A.; Paul, A.; Sen, S. O.; Sen, K. K. *Asian J. Pharm. Sci.* **2015**, *10*, 99–107.

18. Herzberger, J.; Niederer, K.; Pohlit, H.; Seiwert, J.; Worm, M.; Wurm, F. R.; Frey, H. *Chem. Rev.* **2016**, *116*, 2170–2243.

19. Hoare, T. R.; Kohane, D. S. *Polymer.* **2008**, *49*, 1993–2007.

20. Noh, M.; Kang, S.; Mok, Y.; Choi, S. J.; Park, J.; Kingma, J.; Seo, J.-H.; Lee, Y.; Park, T.; Lee, Y. *Chem. Commun.* **2016**, *53*, 509–512.

21. Yoshimitsu, H.; Kanazawa, A.; Kanaoka, S.; Aoshima, S. *Macromolecules* **2012**, *45*, 9427–9434.

22. Patra, L.; Messman, J. M.; Toomey, R.; Paz, Y.; Kishida, A.; Akashi, M. *Soft Matter* **2013**, *9*, 4349.

23. Van Assche, G.; Van Mele, B.; Li, T.; Nies, E. *Macromolecules* **2011**, *44*, 993–998.

24. Shimada, N.; Nakayama, M.; Kano, A.; Maruyama, A. *Biomacromolecules* **2013**, *14*, 1452–1457.

25. Zhu, Y.; Batchelor, R.; Lowe, A. B.; Roth, P. J. *Macromolecules* **2016**, *49*, 672–680.

26. Tian, H.-Y.; Yan, J.-J.; Wang, D.; Gu, C.; You, Y.-Z.; Chen, X.-S. *Macromol. Rapid Commun.* **2011**, *32*, 660–664.

27. Käfer, F.; Liu, F.; Stahlschmidt, U.; Jérôme, V.; Freitag, R.; Karg, M.; Agarwal, S. *Langmuir* **2015**, *31*, 8940–8946.

28. Wu, G.; Chen, S.-C.; Zhan, Q.; Wang, Y.-Z. *Macromolecules* **2011**, *44*, 999–1008.

29. Kuila, A.; Maity, N.; Chatterjee, D. P.; Nandi, A. K. *J. Phys. Chem. B* **2016**, *120*, 2557–2568.

30. Roth, P. J.; Davis, T. P.; Lowe, A. B. *Macromolecules* **2012**, *45*, 3221–3230.

31. Vadgama, P. *Surfaces and interfaces for bio-materials*; Woodhead Publishing: Cambridge, 2005; pp 1-824.

32. Thakur, V. K.; Thakur, M. K. *Handbook of polymers for pharmaceutical technologies*; Scrivener Publishing/ John Wiley and Sons Inc: New Jersey, 2015; pp 1-568.

33. Ducheyne, P.; Healy, K.; Dietmar, E.H.; Grainger, D.W.; Kirkpatrik, C.J. *Comprehensive biomaterials*; Elsevier: Massachusett, 2011; Vol. 1, pp 1-557.

34. Severian D. *Polymeric Biomaterials, Revised and Expanded.* [2nd ed.]; Marcel Dekker Inc: New york, 2002; pp 1-1184.

35. Vasquez, J.M.G.; Tumolva, P. T. *Am. J. Chem.* **2015**, *5*, 60–65.

36. Nagarajan, R. *Amphiphiles: Molecular Assembly and Applications*; ACS Symposium Series: Washington, DC, 2011; Vol. 1070; pp 1-22.

37. Lapteva, M.; Mondon, K.; Möller, M.; Gurny, R.; Kalia, Y. N. *Mol. Pharm.* **2014**, *11*, 2989–3001.

38. De, A.; Bose, R.; Kumar, A.; Mozumdar, S. Targeted Delivery of Pesticides Using Biodegradable Polymeric Nanoparticles; Springer: New york, 2013; pp 1-99.

39. Gusev A.I. Khokhlov A.R Govorun E.N. Glossary of Nanotechnolgy and Related Terms; http://eng.thesaurus.rusnano.com/wiki/article1199. (accessed May 28, 2017).

40. Sedláček, O.; Černoch, P.; Kučka, J.; Konefal, R.; Štěpánek, P.; Vetrík, M.; Lodge, T. P.; Hrubý, M. *Langmuir* **2016**, *32*, 6115–6122.

41. Laing, S.; Suriano, R.; Lamprou, D. A.; Smith, C.-A.; Dalby, M. J.; Mabbott, S.; Faulds, K.; Graham, D. *ACS Appl. Mater. Interfaces* **2016**, *8*, 24844–24852.

42. Mackenzie, K. J.; Francis, M. B. *J. Am. Chem. Soc.* **2013**, *135*, 293–300.

43. Sambath, L.; Kottai Muthu, A.; Kumar, M. A.; Phaneendra, K. *Int. J. Pharm. Sci.* **2013**, 5, 204-210.

44. *BASF, Pharma Ingredients Serv.* **2010**, No. July, 1–22.

45. Reintjes, T. *Solubilty Enhancement with BASF Pharma Polymers Solubilizer* Compedium; **2011**.

46. Feil, H.; Bae, Y. H.; Feijen, J.; Kim, S. W. *Macromolecules* **1993**, *26*, 2496–2500.

47. Hurtgen, M.; Liu, J.; Debuigne, A.; Jerome, C.; Detrembleur, C. *J. Polym. Sci. Part A Polym. Chem.* **2012**, *50*, 400–408.

48. Khokhlov, A. R. *Polymer.* **1980**, *21*, 376–380.

49. Jeong, B.; Kim, S. W.; Bae, Y. H. *Adv. Drug Deliv. Rev.* **2002**, *54*, 37–51.

50. Balzam, R. *MSU Grad. Theses* **2016**.

51. Ohnaga, T.; Sato, T. *Polymer.* **1996**, *37*, 3729–3735.

52. Debuigne, A.; Caille, JR.; Willet, N.; Jérôme, R. *Macromolecules* **2005**, 38, 9488-9496.

53. Ladavière, C.; Lacroix-Desmazes, P.; Delolme, F. *Macromolecules* **2009**, *42*, 70–84.

54. Binder, W. H.; Pulamagatta, B.; Kir, O.; Kurzhals, S.; Barqawi, H.; Tanner, S. *Macromolecules* **2009**, *42*, 9457–9466.

55. Willemse, R. X. E.; Staal, B. B. P.; Donkers, E. H. D.; Van Herk, A. M. *Macromolecules* **2004**, *37*, 5717–5723.

56. Yasushi, M.; Tomoya, N.A.; Ikeda, I. *Macrolecules* **2001**, 35, 217- 222.

57. Tager, A. A.; Safronov, A. P.; Sharina, S. V.; Galaev, I. Y. *Colloid Polym. Sci.* **1993**, *271*, 868–872.

58. Beija, M.; Marty, J.-D.; Destarac, M.; Yang, G.; Hirvonen, J.; Prez, F. Du; Tenhu, H.; Marty, J.-D. *Chem. Commun.* **2011**, *47*, 2826.

59. Yanul, N. A.; Kirsh, Y. E.; Verbrugghe, S.; Goethals, E. J.; Du Prez, F. E. *Macromol. Chem. Phys.* **2001**, *202*, 1700–1709.

60. Choi, J. H.; Ko, S.-W.; Kim, B. C.; Blackwell, J.; Lyoo, W. S. *Macromolecules* **2001**, *34*, 2964–2972.

61. Odian, G. G. *Principles of polymerization,* [3rd ed.]; Wiley: New york, 1991.

62. Park, S. H.; Choi, B. G.; Joo, M. K.; Han, D. K.; Sohn, Y. S.; Jeong, B. *Macromolecules* **2008**, *41*, 6486–6492.

63. Moon, H. J.; Ko, D. Y.; Park, M. H.; Joo, M. K.; Jeong, B.; Song, S. C.; Armes, S. P.; Lewis, A.; MacNeil, S.; Qian, Z. Y.; Jo, S.; Kim, W. J.; Graves, M.; Zhao, X.; Wei, Y. Q. *Chem. Soc. Rev.* **2012**, *41*, 4860.

64. Jeong, B.; Bae, Y.H.; Sung, W. K. **1999**, 32, 7064-7069.

65. Zhang, H.; Yu, L.; Ding, J. *Macromolecules* **2008**, *41*, 6493–6499.